KTH Chemical Science
and Engineering

POLYELECTROLYTE COMPLEXES OF BOTTLE BRUSH COPOLYMERS: SOLUTION AND ADSORPTION PROPERTIES

Alexander Shovsky
(Oleksandr Shovskyy[1])

Doctoral Thesis in Chemistry at the Royal Institute of Technology

Stockholm, Sweden 2011

[1] According to Ukrainian Passport

Akademisk avhandling som med tillstånd av Kungliga Tekniska Högskolan framlägges till offentlig granskning för avläggande av teknologie doktorsexamen onsdagen den 1 juni 2011 kl. 10.00 i hörsal F3, Kungliga Tekniska Högskolan, Lindstedtsvägen 26, Stockholm.

Alexander Shovsky
Title: POLYELECTROLYTE COMPLEXES OF BOTTLE BRUSH COPOLYMERS: SOLUTION AND ADSORPTION PROPERTIES

TRITA-CHE-Report 2011:37
ISSN 1654-1081
ISBN 978-91-7415-998-1

Department of Chemistry
Division of Surface and Corrosion Science
School of Chemical Science and Engineering
Royal Institute of Technology
SE-100 44 Stockholm

Printed at E-PRINT

To my parents (Alexandra Shovskaya and Vladimir Shovsky) who provided the opportunities and to my family (Galyna and Ivan) for their love, support, patience and understanding

List of Papers

This thesis is based on the following six papers, which will be referred to by their roman numerals:

Paper I ***Formation and Stability of Soluble Stoichiometric Polyelectrolyte Complexes: Effects of Charge Density and Polyelectrolyte Concentration***
Shovsky, AV; Varga, I; Makuska, R; Claesson, P.M.
Journal of Dispersion Science and Technology **2009**, *30*, 6, 980-988

Paper II ***Formation and Stability of Water-Soluble, Molecular Polyelectrolyte Complexes: Effects of Charge Density, Mixing Ratio, and Polyelectrolyte Concentration***
Shovsky, A; Varga, I; Makuska, R; Claesson, P.M.
Langmuir **2009**, *25,* 11, 6113-6121

Paper III ***Adsorption characteristics of brush polyelectrolytes on silicon oxynitride revealed by dual polarization interferometry***
Bijelic, G; Shovsky, A; Varga, I; Makuska; R; Claesson, P.M.
Journal of Colloid and Interface Science **2010,** 348, 1, 189-197

Paper IV ***Adsorption Characteristics of Stoichiometric and Nonstoichiometric Molecular Polyelectrolyte Complexes on Silicon Oxynitride Surfaces***
Shovsky, A; Bijelic, G; Varga, I; Makuska, R; Claesson P.M.
Langmuir **2011**, 27(3), 1044–1050

Paper V ***Adsorption Characteristics of Molecular Polyelectrolyte Complexes on Silicon Oxynitride Surfaces: Effect of Molecular Weight, Stoichiometry and Concentration***
Shovsky, A; Varga, I; Makuska, R; Claesson, P.M.
Soft Matter, Submitted, **2011**

Paper VI ***Cationic PNIPAAM Block Copolymer Adsorption on Silicon Oxynitride: Effects of the Length of the Charged Block***
Shovsky, A; Knohl; S, Dedinaite, A.; Zhu K; Kjøniksen, A.-L.; Nyström, B; Linse, P.; Claesson, P.M.
Manuscript

The author's contributions to the papers are as follows:

Paper I-II and **Paper IV-VI**: major part of planning, experimental work and data analysis. Major part of manuscripts was written by thesis author.
Paper III: part of experimental work and part of data analysis.

Other papers by the author

- Adsorption Kinetics of Molecular Polyelectrolyte Complexes on Silicon Oxynitride Surfaces: Effect of Molecular Weight, Stoichiometry and Concentration
  Shovsky, A; Varga, I; Makuska, R; Claesson, P.M.
  Manuscript
- Organic and macromolecular films and assemblies as (bio)reactive platforms: From model studies on structure-reactivity relationships to submicrometer patterning
  Schonherr, H; Degenhart, GH; Dordi, B, Shovsky, A; et al.
  Ordered Polymeric Nanostructures at Surfaces **2006**, *200*, 169-208
- Dip-pen nanolithography on (bio)reactive monolayer and block-copolymer platforms: Deposition of lines of single macromolecules
  Salazar, RB; Shovsky, A; Schonherr, H, et al.
  Small, **2006**, *2*, 11, 1274-1282
- AFM tip mediated nanofabrication of (bio) reactive polymer platforms: Towards deposition of single dendrimer molecules onto reactive films
  Schonherr, H; Salazar, RB; Shovsky, A, et al.
  Abstracts of Papers of The American Chemical Society, **2006**, *231*, 192
- New combinatorial approach for the investigation of kinetics and temperature dependence of surface reactions in thin organic films
  Shovsky, A; Schonherr, H
  Langmuir, **2005**, *21*,10, 4393-4399
- Patterned reactive macromolecular thin film platforms at the interface between sensors and biological systems.
  Schonherr, H; Feng, C; Shovsky, A, et al.
  Abstracts of Papers American Chemical Society, **2005**, 229, U62

- New combinatorial approach for the investigation of kinetics and the temperature dependence of surface reactions in thin organic films
  Schonherr, H; Shovsky, A; Vancso, GJ
  Abstracts of Papers of The American Chemical Society, **2005**, *229* U700-U700
- Interfacial reactions in confinement: Kinetics and temperature dependence of reactions in self-assembled monolayers compared to ultrathin polymer films
  Schonherr, H; Feng, CL; Shovsky, A
  Langmuir, **2003**, *19*, 26, 10843-10851
- Reactive macromolecular films for biomolecule immobilization: Fabrication of sub-micrometer reactive patterns and impact of confinement on reactivity
  Schonherr, H; Feng, C; Shovsky, A, et al.
  Abstracts of Papers American Chemical Society **2004**, *227*, U550
- Interfacial reactions in confinement: Kinetics and temperature dependence of reactions in self-assembled monolayers compared to ultrathin polymer films
  Schonherr, H; Feng, CL; Shovsky, A
  Abstracts of Papers of The American Chemical Society, **2003**, *226*, U484-U484

Abstract

The aim of this thesis work was to systematically investigate the physico-chemical properties of polyelectrolyte complexes (PECs) formed by bottle brush and linear polyelectrolytes in solution and at solid / liquid interfaces. Electrostatic self-assembly of oppositely charged macromolecules in aqueous solution is a versatile strategy to construction of functional nanostructures with easily controlled properties. Bottle brush architecture, introduced into the PEC, generates a number of distinctive properties of the complexes, related to a broad range of application, such as colloidal stability and protein repellency to name a few. To utilize these materials in a wide range of applications e.g. drug delivery, the understanding of the effects of polymer architecture and solution parameters on the properties of bottle brush PECs is of paramount importance.

This thesis constitutes a systematic investigation of PECs formed by a series of cationic bottle-brush polyelectrolytes and a series of anionic linear polyelectrolytes in aqueous solution. The focus of the first part of the thesis was primarily on formation and characterization of PECs in solution, whereas the adsorption properties and adsorption kinetics of bottle-brush polyelectrolytes and their complexes was investigated in the second part of the thesis work. In particular, effects of the side-chain density of the bottle-brush polyelectrolyte, concentration, mixing ratio and molecular weigh of the linear polyelectrolyte on formation, solution properties, stability and adsorption of PECs were addressed.

The pronounced effect of the side-chain density of the bottle-brush polyelectrolyte on the properties of stoichiometric and nonstoichiometric PECs was demonstrated. Formation of PECs by bottle-brush copolymers with high density of side-chains results in small, water-soluble, molecular complexes having nonspherical shape, independent of concentration. Whereas formation of PEC-aggregates was revealed by bottle-brush polyelectrolytes with low side chain density, the level of aggregation in these complexes is controlled by polyelectrolyte concentration. The structure of the PECs formed with low molecular weight polyanions is consistent with the picture that several small linear polyelectrolyte molecules associate with the large bottle-brush. In contrast, when complexation occurs between polyanions of high molecular weigh and the bottle-brush polymers considerably larger PECs are formed, consistent with several bottle-brush polymers associating with one high molecular weight polyanion.

Adsorption kinetics and properties of stoichiometric and nonstoichiometric PECs on negatively charged silicon oxynitride were investigated. PECs formed by low charge density bottle-brush polyelectrolytes adsorbed in larger amount and formed thicker layers compared to complexes formed by higher charge density bottle-brush copolymers, regardless of stoichiometry and concentration. In general, the adsorbed amount decreases with increasing polyion content of the complex, and at a given polyion content with the molecular weight of the polyanion. Further, the thickness of the layer formed scales with the adsorbed amount, independent of polyanion molecular weight. This finding is rationalized by removal of polyanion from the complex during the adsorption event. The adsorbed mass achieved under a given condition is thus dictated by a competition between anionic surface sites and anionic sites on the polyanion for complexation with the cationic sites on the bottle-brush.

This dissertation work also addressed adsorption of diblock polyelectrolytes, composed of one cationic block and one non-ionic block, where different lengths of the charged block was considered. It was shown that adsorption of the block-copolymers is primarily driven by electrostatics, but the non-electrostatic affinity between the non-ionic block and silica oxynitride does also contribute. The adsorbed mass increased and passed a maximum when the length of charged block was increased. For small cationic blocks the adsorption is limited by repulsion between the non-ionic chains, whereas electrostatic interactions limit the adsorption of diblock polyelectrolytes with a large cationic block.

Key-words: Polyelectrolyte complex, bottle-brush polymer, block polyelectrolyte, light scattering, electrophoretic mobility, turbidity, colloidal stability, adsorption, adsorption kinetics, dual polarization interferometry

Summary of Papers

Formation and properties of sterically stabilized polyelectrolyte complexes (PEC) with stoichiometric composition formed between a series of bottle brush polyelectrolytes PEO_{45}MEMA:METAC-X, where X is the mol% of main-chain segments that carries a positive charge with the remaining main-chain segments (1-X) carrying a 45 unit long PEO_{45} side chain, and oppositely charged linear $NaPSS_{4300}$ (4300 is the molecular weight of the PSS) were investigated in **Paper I**. Dynamic and static light scattering and electrophoretic mobility techniques were used. The pronounced effect of the PEO_{45} side-chain density of the brush polyelectrolyte on the properties of stoichiometric PECs was demonstrated. Formation of PECs by brush copolymers with high density of PEO_{45} side chains ((1-X) = 75, 50) results in small, water-soluble, molecular complexes having nonspherical shape, independent of concentration. PEC-aggregates formed by brush polyelectrolytes with low ((1-X) = 25) PEO_{45} density form turbid colloidal dispersions, whose level of aggregation is controlled by the polyelectrolytes concentration. Insoluble complexes were revealed for the PEO_{45}-free METAC/ NaPSS system.

In **Paper II** the above study was extended to consider the formation of nonstoichiometric PECs. The same set of techniques as in **Paper I** was employed. Large colloidally stable aggregates of nonstoichiometric complexes, negatively (1:2) and positively (2:1) charged, were formed in the presence of a relatively small amount of PEO_{45} side chains ((1-X) = 25) in the cationic brush copolymer. (The notation (1:2) is the ratio of cationic polyelectrolyte charges, first number, to anionic polyelectrolyte charges, second number, added to the mixed solution). These PECs are sterically stabilized by the PEO_{45} chains. By further increasing the PEO_{45} side-chain content ((1-X) = 50 and 75) in the cationic copolymer, small, water-soluble molecular complexes could be formed. Regardless of PEO_{45} content, the size of the complexes decreases in the order (1:2) > (1:1) > (2:1). The data suggest that PSS molecules and the charged backbone of the cationic brush form a compact core, and with sufficiently high PEO_{45} chain density molecular complexes are formed that are stable over prolonged times.

The main focus of **Paper III** is on adsorption properties of bottle-brush polyelectrolytes in water investigated on silicon oxynitride by dual polarization interferometry (DPI). The results demonstrate how adsorbed amount, thickness, and refractive index of the adsorbed

polymer layers, and the adsorption kinetics parameters, depend on the PEO_{45}MEMA:METAC-X architecture, i.e. the ratio between backbone charges and side chains. It was shown than both the cationic groups and the PEO side chains have affinity for siliconoxynitride surfaces, and thus contribute to the adsorption process that becomes rather complex. Based on these results and existing polymer adsorption theory, an adsorption mechanism was proposed that involves competitive adsorption of PEO side chains and charged main-chain segments.

Paper IV deals with the adsorption properties of PEO_{45}MEMA:METAC-X / $NaPSS_{4300}$ complexes in aqueous solution investigated by DPI. The effect of polyanion PSS content on the PEC adsorption was the main focus. The chemical composition of the adsorbed layers was estimated from X-ray photoelectron spectroscopy (XPS) measurements. A pronounce effect of PSS content on adsorbed amount and layer thickness was revealed. An adsorption mechanism based on electrostatic interactions and side-chain affinity was invoked, and extended to consider the competition between PSS and anionic surface sites for binding to the cationic sites of the bottle-brush polyelectrolyte. Regardless of complex composition, some desorption of the anionic component of the PEC upon layer formation was suggested by the XPS results. Thus, the composition in the adsorbed layers is different from the solution composition, and strongly dominated by the cationic bottle-brush polymer.

The solution and adsorption properties of stoichiometric and non-stoichiometric PEO_{45}MEMA:METAC-X / NaPSS complexes, f ormed by linear anionic polyelectrolytes with different molecular weight were investigated in **Paper V**. The properties of the PEC were determined by DLS and electrophoretic mobility measurements, whereas the adsorption of complexes on silicon oxynitride was investigated using DPI. It was demonstrated that cationic, uncharged and negatively charged complexes all adsorb to negatively charged silicon oxynitride, and maximum adsorption was achieved for positively charged complexes containing small amounts of PSS. For any given stoichiometry, the adsorbed amount was found to decrease with increasing molecular weight of PSS. The adsorption kinetics was also reduced with increasing PSS content and PSS molecular weight. An adsorption mechanism was suggested based on analysis of adsorbed layer characteristics. The thickness of the layer was found to scale with the adsorbed amount, and the same master curve was observed independent of PSS molecular

weight. This finding is rationalized by removal of PSS from the complex during the adsorption event. The adsorbed mass achieved under a given condition is thus dictated by a competition between anionic surface sites and anionic sites on PSS for complexation with the cationic sites on the bottle-brush. This equilibrium is shifted towards the complex side with increasing PSS content and increasing PSS molecular weight.

Paper VI deals with adsorption of diblock copolymers composed of one cationic and one non-ionic block with the following composition poly(*N*-isopropyl acrylamide)$_{48}$ - *block*-poly((3-acrylamidopropyl)-trimethyl ammonium chloride)$_X$, where the subscripts denote the mean degree of polymerization for each block and X = 0, 6, 10, 14, 20. These polymers are referred to as PNIPAAM$_{48}$-*b*-PAMPTMA(+)$_X$. The adsorption was investigated on silicon oxynitride by DPI. It was demonstrated that both the cationic and non-ionic (temperature responsive) blocks exhibit affinity to silicon oxynitride and thus both contribute to the adsorption process. The maxima in adsorbed mass and film thickness were obtained for PNIPAAM$_{48}$-*b*-PAMPTMA(+)$_{10}$, whereas minimum values of these characteristics were found for PNIPAAM$_{48}$ and PNIPAAM$_{48}$-*b*-PAMPTMA(+)$_{20}$ respectively. For larger cationic blocks the adsorption is limited electrostatic repulsion, whereas steric repulsion between the PNIPAAM chains limited the adsorption process for short cationic blocks.

C O N T E N T S

1. INTRODUCTION

Over the past several decades, polymer chemistry has developed diverse synthetic strategies capable to create novel macromolecules of various topologies. Bottle brush copolymers represent a versatile class of macromolecular architectures, consisting of side chains grafted to a main chain. Structural factors of the macromolecular architecture, like the graft density and length of the side chains and the charge density of the backbone can be accurately controlled.

Construction of supra-molecular structures using lower molecular weight compounds as building blocks has received great attention. The ultimate goal is to produce preprogrammed hierarchical structures of functional materials. The hierarchy can be achieved by inserting "information" in the building blocks in the form of hydrophobic/hydrophilic character, electrostatic interaction etc. that is used for self-assembly of the compounds into the superstructures. A common pair of building blocks that have been investigated intensively over the past years is comprised of oppositely charged polyelectrolytes in aqueous solutions. The main interactions that take place in such systems are electrostatic interactions between the charges of the oppositely charged polyelectrolytes, which results in the formation of polyelectrolyte complexes (PECs), often with limited colloidal stability. This limitation can be overcome by employing polyelectrolytes with bottle brush architecture. The molecular design of such bottle brush copolymers consisting of various polyelectrolyte backbones and water-soluble nonionic side-chains provides a flexible strategy to prepare a large variety of novel water-soluble PECs. Thus, there is a need for a more thorough understanding on the effect of system parameters on the self-assembly and properties of bottle brush PECs. It is therefore both fundamentally and practically important to understand how a conformationally rigid bottle brush polyelectrolyte interacts electrostatically with oppositely charged macromolecules and surfaces.

Electrostatic self-assembly of macromolecules provides an efficient and rapid pathway for the synthesis of objects from nanometer to micrometer range that are difficult if not impossible to obtain by conventional chemical reactions. Depending on the morphologies of the PECs obtained (size, shape, periodicity, etc.) these nano-assemblies have already been applied, or shown to be suitable for, a number of applications in nanotechnology, reusable materials, electronics and drug delivery.

2. MACROMOLECULAR SYSTEMS

2.1 POLYELECTROLYTES

Polyelectrolytes are charged polymers that are common in biological systems, industrial settings, and everyday life.[1] The term polyelectrolyte is employed for polymers consisting of a macroion, i.e., a macromolecule carrying covalently bound anionic or cationic groups, and low-molecular weight counterions.[2] In generally accepted terminology the polymers carrying positive and/or negative charges are referred to as polyelectrolytes, macroions, polyions or ionic polymers. The interference of polymer and electrolyte character in one entity has generated considerable interest and opened new areas of novel applications.[3]

In the solid state as well as in apolar solvents, the counterions are strongly bound to the polymer ion groups, and the chains have no net charge. Dissolving a polyelectrolyte in a polar solvent leads to dissociation of the ion pairs. In contrast to the localized charges along the chain, the counterions may redistribute in the whole sample volume thereby charging the polyelectrolyte (Figure 2.1a). In aqueous solution, the polymer coils are greatly expanded by the presence of charged groups. This occurs due to the strong electrostatic repulsion between charged backbone segments. If the solution is free of added electrolytes, the polymer coil expands as the polymer concentration decreases. This is known as "polyelectrolyte effect".[4] Many properties, like chain conformation, diffusion coefficient, solution viscosity, polarisability, miscibility etc. are drastically altered if ionic groups are introduced. In presence of high amounts of added electrolytes, the polyelectrolytes behave like non-ionic polymers and chain expansion is no longer observed.[5] Another typical feature of polyelectrolytes is a low activity coefficient of the counter ions. If the charge density of the polyelectrolyte is high enough a fraction of the counterions condenses at the ‘surface’ of the macroion.[6, 7] The physical background of the counterion condensation phenomenon is the competition between a gain in energy due to electrostatic interactions and a loss of entropy due to counterion confinement.[8]

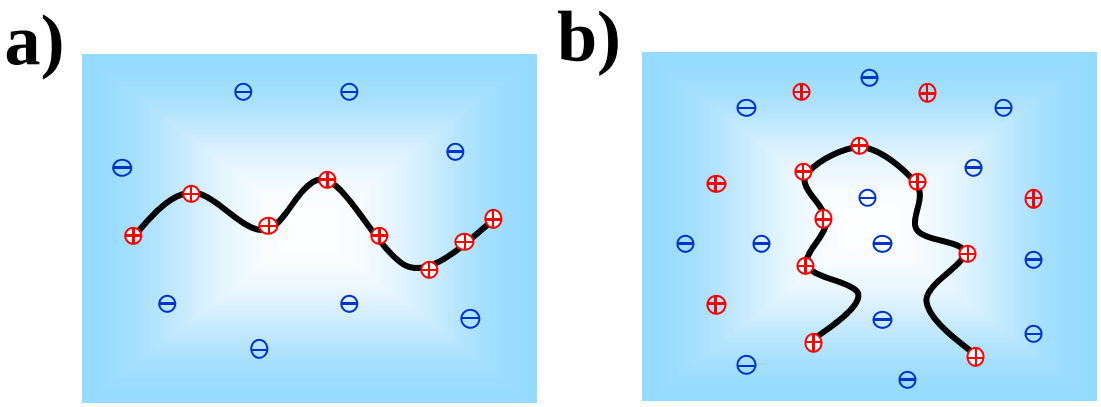

Figure 2.1 *Scheme of polyelectrolyte chain in a) water and b) aqueous salt solution e.g. NaCl; a) chain configuration is expanded by electrostatic and solvent interactions b) coiling of chain induced by addition salt due to reduction of electrostatic repulsion between charged units within chain. Further addition of salt may lead to collapsed globule conformation if the solvent interactions are unfavorable.*

The conformation of a polyelectrolyte in solution is determined by the minimum of free energy.[9] To reduce the number of unfavorable polymer-solvent-contacts in poor solvent, uncharged chains collapse to dense globules, which minimize the contact area. The size of the polymer coil depends on the solvent and on the molecular weight of the polymer. In contrast the conformation of a charged polymer is determined by the balance of electrostatic repulsion, entropy elasticity of the chain, entropy of the counterions, and solvent-solute interactions.[10] A simple characteristic of the polyelectrolyte coil is the mean distance between the polymer ends, R_m. Another measure of the polymer chain size is the radius of gyration, R_g, which describes the average distance of polymer segments from the centre of mass of the macromolecule.

The polyelectrolytes may be categorized according their origin into synthetic, natural or modified.[11] Biomacromolecules, such as (carriers of information) nucleic acids DNA and RNA, (metabolism-machines) like proteins, structural elements e.g. charged polysaccharides, cellulose or pectin, and energy storage e.g. starch are natural polyelectrolytes, while poly(diallyl dimethyl ammonium chloride), PDADMA, and poly(styrene sulfonic acid), PSSA, are examples of synthetic polymers.

Polyelectrolytes may also be classified according to the nature of their bound ions, specifically type of ion, amount of ion present along a given length of polymer chain, type of counterion ((a)univalent (b) divalent or trivalent (c) polymeric) etc. The bound ion can be either cationic or anionic; in some cases both types can occur together

(ampholytic). In each case the polyion may be strong or weak according to how the degree of ionization is affected by pH-changes. Strong polyelectrolytes, poly-salts, e.g., sodium-polystyrene-sulfonate, dissociate completely in the total pH range accessible by experiment. The total charge as well as its specific distribution along the chain is solely imposed by the polymer structure. (In this thesis strong polyelectrolytes have been considered). On the other hand, weak polyelectrolytes (polyacids and polybases), such as e.g. polyacrylic acid or polyethylene amine, have a degree of dissociation that depends on pH.[12] Yet another classification distinguishes between integral and pendant polyelectrolytes, differing in the positions of their ionic groups in the polymer chain: back bone or side chain.[13]

Many applications of polyelectrolytes are based on their abilities to modify the fluid properties of an aqueous medium or modifying the behavior of particles in aqueous slurries or colloidal suspension. Polyelectrolytes increase the viscosity of aqueous solutions and act as thickeners in e.g. puddings or creamy low fat milk products in food industry, pharmaceutical products and latex paints, creams and ointments in cosmetics industry and all kinds of hair products.[1] Furthermore, they are applied as flocculation agents for cellulose/paper production,[14] for waste water processing[15] or for the precipitation of colloids from solution in various processes.[16, 17] Polyelectrolytes can also stabilize particles in aqueous suspension thus acting as dispersants[18] and they have been shown to be suitable as adhesion modifiers.[19] Other applications are the usage as additives for spinning fibers in textile industry, as viscosity modifier to reduce drag in oil pipelines, as superabsorbent polymers used in hygiene products, or the production of ion exchange resins.[5, 12, 20] In addition to that, assembling these polyelectrolytes into ultra thin film composite membranes is one of the most important applications and has received significant attention and interest.[21-23]

2.2 BLOCK POLYELECTROLYTES

A block copolymer may be defined as a macromolecule which consists of two or more chemically different regions.[24] In the simplest case, a diblock copolymer AB consists of two different homopolymers (covalently) linked end to end. The properties of block copolymers depend on chemical nature, relative amount and structure of repeating monomer units that form the constituent homopolymers, as well as on the various

environmental parameters, such as e.g. pH, temperature, concentration etc. The ability of block copolymers to self-assemble, both in solution and in bulk, and to generate a variety of microdomain morphologies (lamellae, hexagonally packed cylinders, body-centered cubic (bcc) spheres, gyroids, etc.) is well documented.[25]

Block copolymers containing charged segments are termed polyelectrolyte block copolymers, also known as ionic block copolymers.[26] This class of macromolecules combines properties of polyelectrolytes, block copolymers and surfactants.[27] A distinctive feature of block polyelectrolytes is the ability to self-assemble in solution in a selective solvent, i.e., a solvent that is good for one block and poor for the other.[28] The self assembly results in the formation of stable micelles in a great variety of structures (morphologies).[29] The self-assembly can be controlled by varying the ionic strength, solvent quality, or degree of polymerization of the blocks. Micellization occurs when the block copolymer is dissolved in a large amount of a selective solvent for one of the blocks. Under these circumstances, the polymer chains tend to organize themselves in a variety of structures from micelles or vesicles to cylinders.

The major driving force for the self assembly of polyelectrolyte copolymers is the decrease in free energy of the system due to the segregation of the hydrophobic fragments from the incompatible aqueous environment by the formation of a micelle core stabilized and 'shielded' from the surrounding aqueous media by the 'corona' formed by ionic blocks.[30] The charged corona provides to the micelle solubility in aqueous media (i.e., "dispersion stability").

The ability of a macromolecule to respond to external stimuli, such as pH,[31] light[32] and temperature[33] is termed as stimuli responsiveness. The response of a macromolecule to an external stimulus is often accompanied by a sharp conformational change as well as changes in physical properties. Block copolymers with stimuli-responsiveness have been extensively investigated, partly due to interesting fundamental questions involved when trying to understand these systems, and partly due to a great number of possible applications in nanotechnology.[34] The results have been summarized in several excellent reviews.[31, 35-37] Muller et al.[38] reported on the properties of PAA-b-poly(N,N-diethylacrylamide). Poly(N,N-diethylacrylamide) exhibits a lower critical solution temperature (LCST of 32 °C), whereas the degree of ionization of PAA can be controlled by pH change. Depending on pH and temperature, these polymers can form micelles, inverse micelles or hydrogels.[39] Therefore, this ionic block copolymer can be used for

potential therapeutic applications, e.g., controlled drug delivery based on temperature/pH-triggered release.

Ionic block copolymers have received much interest in numerous applications such as drug delivery and release systems in medicine,[40-42] membranes in separation technology and fuel cells,[43] flocculants in waste water treatment[44] and stabilizers.[45]

2.3 BOTTLE BRUSH POLYELECTROLYTES

Molecular brushes represent a special class of graft copolymers, composed of a main chain (backbone) and densely grafted side chains.[46] Recent advances in synthetic polymer chemistry have provided an opportunity to produce cylindrical polyelectrolyte brushes, i.e. polymer chains, densely grafted with multiple polylectrolyte chains, or a polyelectrolyte backbone grafted with non-ionic polymer chains.[47] These so-called "bottle-brush copolymers", also known as comb-like copolymers, exhibit an interesting competition due to the steric repulsion between the side chains and the configurationally entropy of the backbone: varying the grafting density of the side chains and their length, the effective stiffness of these cylindrical brushes can be controlled over a wide range.[48] If the length of the backbone is significantly longer than that of the side chains, intramolecular excluded volume effects cause the polymer to adopt a cylindrical shape with the backbone polymer in the core from which the side chains emanate radially.[49] Conversely, molecular brushes with backbones on the order of the length of the side chains generally adopt compact, spherical dimensions that resemble star polymers.[50]

Molecular brushes can be classified with respect to the chemical composition of the side chains as i) homopolymer brushes (Figure 2.2a) and ii) random/block copolymer (Figure 2.2b,c) brushes. Recently, more sophisticated architectures, termed as brush on brush, have been reported (Figure 2.2d).

Synthetically, a variety of approaches have been adopted to allow the preparation of bottle brushes. Generally, there are three strategies employed for the synthesis of molecular brushes: "grafting through" (polymerization of macromonomers),[51] "grafting to" (attachment of the side chains to the backbone),[52] and "grafting from" (grafting the side chains from the backbone).[53] The grafting through route involves the polymerization of macromonomers - polymers with polymerizable end groups – "through" their terminal

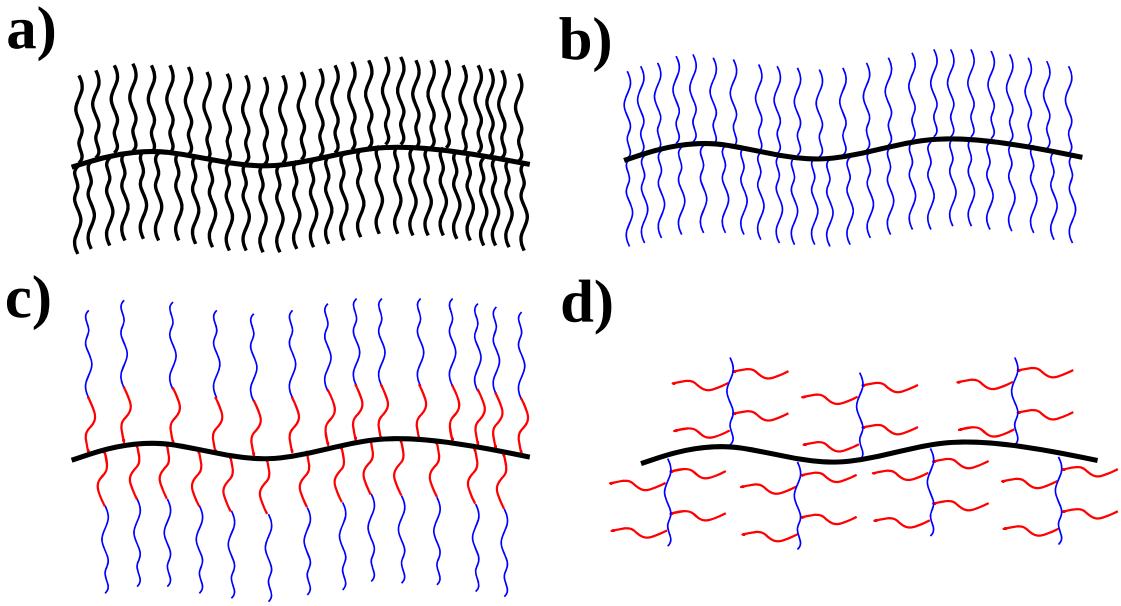

Figure 2.2 *Schematic representation of bottle brush structures with different side chains a) homopolymer b) copolymer c) block-copolymer d) brush-on-brush.*

functionality. This method allows the preparation of brushes with 100% grafting density. It is difficult, however, to synthesize molecular brushes with a high degree of polymerization (DP) and low polydispersity because of the inherently low concentration of polymerizable groups and the steric hindrance imposed by the side chains.[54, 55]

A fascinating aspect is also the importance of bio-macromolecules with bottle-brush architecture, such as proteoglycans[56, 57] and glycoproteins[57]. These polyelectrolytes consist of a protein backbone and carbohydrate side chains, performing biological functions from cell signaling and cell surface protection to joint lubrication.[58] Proteoglycans, e.g. aggrecan[59] and the mucins,[60] can be found on vast variety of cells. These biological brush polyelectrolytes remain one of the least well understood biopolymer systems in molecular biology and currently they are the subject of intense investigation.[61] Molecular brushes have been proposed as synthetic substitutes for natural proteoglycans in order to better understand the architecture-property relationship, which could potentially lead to advances in biomedical applications. Nontoxic bottle-brush brush structures as biomimetic functional soft interfaces between solid semiconductors and biological systems may find direct applications for designing advanced biomedical devices.[62]

2.4 POLYELECTROLYTE COMPLEXES

In this section polyelectrolyte complex formation, properties and applications are reviewed. The emphasis is put on the factors investigated in this thesis, i.e., the charge density of the polyelectrolytes, molecular weight, the mixing ratio and ionic strength.

2.4.1 Introduction

Polyelectrolyte complexes (PECs) are referred to a class of polymeric compounds consisting of oppositely charged polyions.[63] Complex formation between synthetic anionic and cationic polyelectrolytes has been a well-known phenomenon for more than 60 years.[64] Mixing aqueous solutions of anionic and cationic polyelectrolytes results in a spontaneous formation of polyelectrolyte complexes (PECs), also known as polyion complex (PICs).[65] A completely different approach leading also to highly ordered polymer complexes is the (template) polymerization of monomers along macromolecules.

In general, electrostatically driven assembly enables formation of complexes between polyelectrolytes and surfactants,[66] colloidal particles,[67] biomacromolecules,[68] and, in particular, oppositely charged polyelectrolytes. Formation of PECs is a result of cooperative coupling reactions between two oppositely charged regions of polyions. The nano-particles formed demonstrate entirely new properties, remarkably different from those of the constituting polyelectrolytes.[69] Thus, PECs represent a special class of macromoleculecular systems possessing versatile and easily tailored compositions and structures in solution.

2.4.2 Complexation Process

The formation of PECs is predominantly driven by strong electrostatic interactions between the oppositely charged macromolecules and by liberation of small counterions as well as a number of water molecules from the hydration shell around the polymers.[70] However, hydrogen bonding, hydrophobic interactions and van der Waals forces, or combinations of these interactions, usually contribute to complex formation. The process of PEC formation is athermal or nearly ideal ($\Delta H=0$).[65] However, several studies have

demonstrated that the process of PEC formation can be either endothermal ($\Delta H < 0$) or exothermal ($\Delta H > 0$).[71] With increasing ionic strength, ΔH decreases which is caused by the salt screening effect. From the thermodynamic point view ($\Delta G = \Delta H - T\Delta S$), the formation of polyelectrolyte complexes is driven by the gain of entropy ($\Delta S > 0$).[70] Thus, the favorable association is rather entropic in origin and not enthalpy driven. The entropic nature of polyelectrolyte association was recognized many decades ago. For example, Michaels and co-workers[72] ascribe the mixing to be driven by "the escaping tendency of microions."

A polyelectrolyte chain in aqueous solution is typically enshrouded by a (low molecular weight) counterion cloud where the number of condensed counterions within such cloud increases with polyelectrolyte charge density but decreases with the polarity (dielectric constant) of the solvent.[73] During complexation with a polyelectrolyte chain, incoming molecules have to compete with and displace condensed counterions. Thus, the liberation of counterions leads to entropy increase and facilitates the complexation process, provided that the entropy increase upon ion release exceeds the entropy decrease upon collapse and condensation of the polyelectrolytes.

2.4.3 Structure of Polyelectrolyte Complexes

Two major steps dictate PEC complexation:[74] (1) the kinetic diffusion process of mutual entanglement between polymers, which occurs at relatively short times and depends on molecular size differences, stereo-chemical fitting, and (2) thermodynamic rearrangement of the already formed simplex aggregate due to conformational changes and disentanglement. The latter process occurs at rather long times leading to a source of instability in the PEC, and it is a consequence of phase separation in aqueous medium. Stop flow measurements have shown that the PEC formation takes place in less than 5 ms, nearly corresponding to the diffusion-controlled collision of polyion coils.[75]

Two structural models for PECs are discussed in the literature, dictated by the characteristics of the polyion groups, stoichiometry, and molecular weights. (i) The ladder-like structure (Figure 2.3a), where complex formation takes place on a molecular level via conformational adaptation. The ladder-like structure consists of hydrophilic single-stranded and hydrophobic double-stranded segments. These phenomena result from the mixing of polyelectrolytes having weak ionic groups and large differences in

molecular dimensions. (ii) Scrambled-egg model (Figure 2.3b), where a large number of chains are incorporated into the particle architecture.

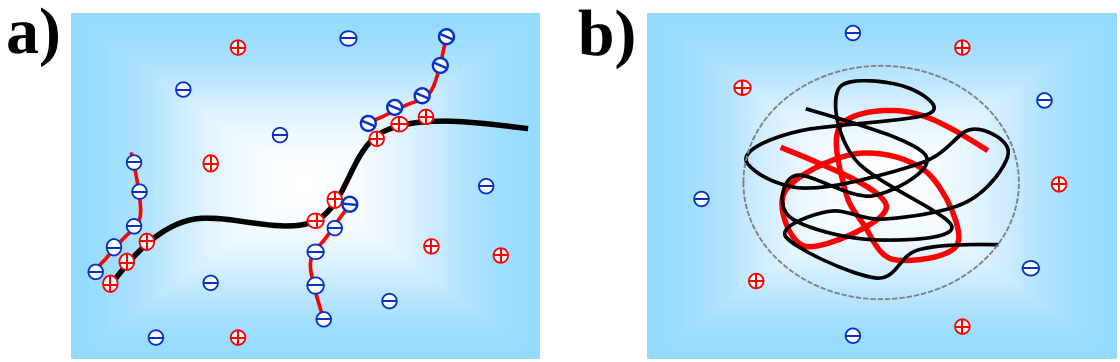

Figure 2.3 *Schematic representation of a) ladder and b) scrambled egg structures. Black represents the large positively charged polyelectrolyte while red represents a polyion of opposite charge (negative); a) shows the ladder representation where insufficient ion pairing occurs under certain stoichiometric conditions leading to macromolecular aggregates, insoluble, and soluble PECs, b) demonstrates the scrambled egg model where polymers of comparable size form complexes yielding insoluble PECs under certain conditions.*

The scrambled-egg model refers to complexes that are the product of the combination of polyions with strong ionic groups and comparable molar masses yielding insoluble and highly aggregated complexes under strict 1:1 stoichiometry.

2.4.4 Factors Influencing Polyelectrolyte Complex Formation

PEC formation is governed by numerous factors, such as the (intrinsic) characteristics of the precursors, e.g. nature, strength and position of ionic sites, charge density, the ratio between numbers of oppositely charged groups of polyelectrolytes, architecture and rigidity of polymer chains, molecular weight as well as the chemical environment, such as solvent, ionic strength, pH, temperature, concentration etc.[63, 74] Properties of PECs have been investigated for many years and the role of some of the parameters is understood. The combination of these parameters is expected to produce complexes with many interesting properties with potential applications.

2.4.5 Stoichiometric and Nonstoichiometric Complexes

Pioneering work by Fuoss and Sadek in 1949, described the complex formation between strong polyelectrolytes poly(sodium styrenesulfonate) and poly(vinyl-N-butylpyridiniumbromide).[64] An important point in describing these PECs is their stoichiometry, i.e. the molar ratio of cationic to anionic groups in the polyelectrolyte components. In the early 1960s Michaels et al. carried out the first systematic studies on formation and properties of PECs with strong synthetic polyelectrolytes. They demonstrated that the mixing of poly(sodium styrene sulfonate) and poly(vinylbenzyltrimethylammonium) chloride yielded an insoluble precipitate containing almost exactly stoichiometric proportions of its components.[65, 72] Stoichiometric PECs contain equal amounts of opposite charges, so that the total charge of such PEC is zero, and they usually phase separate macroscopically. It was emphasized that the combination of the polymer and electrolyte character in PECs produces new materials with unique properties. This new class of ionic materials was shown to be infusible and insoluble in all common solvents, and thus found various applications on a large industrial scale, e.g. hydrophilic soil binders, slag waste, membranes.[76]

While in earlier work the (1:1) stoichiometry of PECs was considered, the deviations from this (1:1) stoichiometry and the development of soluble PECs attracted significant interest in the 1970s, and stressed for the first time in the work of Tsuchida.[77] Comprehensive systematic experimental studies on formation and structure of soluble nonstoichiometric PECs were undertaken by the groups of Kabanov,[78-81] Tsuchida[82] and later on by Dautzenberg,[83-87] whereas theoretic studies were performed by the groups of Khokhlov[88-91] and Linse.[92, 93] The synthetic PECs can be divided into four subclasses by a combination of strong and weak polyelectrolytes.[94, 95] These studies showed that under appropriate salt conditions, the complex formation between polyions with weak ionic groups and significantly different molecular weight in non-stoichiometric systems resulted in soluble complexes. In addition, the preparation and mechanism of the stable polyelectrolyte complex nanoparticles with defined size and shapes were demonstrated by using centrifugation.[96-98]

A generally accepted classification of nonstoichiometric, synthetic PECs has emerged from these studies. They are divided into two categories. (i) Highly aggregated complexes: these PECs are large non-equilibrium aggregates of several polyelectrolyte chains. The formed PEC particles are stabilized by the polyion in excess that charges the

PEC surface and prevents macroscopic precipitation. (ii) Water-soluble molecular complexes: the formation of water-soluble PECs is an equilibrium phenomenon that can occur when the following special conditions are met:[92] (1) one component has weak ionic groups, (2) there is a significant difference in the molecular weights of the oppositely charged chains, (3) the mixture contains a high excess of the long-chain component, and (4) some salt is present in the system. The formation of soluble complexes is governed by thermodynamic equilibrium and results in a uniform distribution of the short chain component among the chains of the oppositely charged long-chain component. If one or more of the above conditions are not met, complex formation results in highly aggregated complex particles in the colloidal range.

2.4.6 Effect of Polyelectrolyte Topology on Complex Properties

Considerable amount of work have been reported by a great number of research groups regarding the influence of various parameters on structure, formation and properties of PECs formed by assembly of liner polyelectrolytes, whereas the effect of topology of the polymeric components has been less studid.[99] Evidently, this is due to the difficult synthesis of these structures which have only been overcome with the advent of controlled polymerization techniques.[51] Polyelectrolyte chain topology is thought to have an influence on the complexation process as well as on the properties of the resulting polymeric assemblies.[74]

Ionic dendrimers representing regularly branched treelike structures have been mostly used as polyelectrolyte with nonlinear structure, and their complexation with oppositely charged macromolecules, both synthetic and natural, has been investigated.[100, 101] At the same time, the interaction of other nonlinear ionic polymers, such as star-shaped polyelectrolytes,[102] hyperbranched polyelectrolytes[103] and in particular, bottle brush polyelectrolytes has received only little attention, however several contributions have been reported recently.[102, 104-109]

For instance, Sotiropoulov et al.[104] reported formation of stoichiometric water-soluble PECs formed upon mixing of dilute solutions of poly(sodium acrylate-co-sodium 2-acrylamido-2-methyl-1-propanesulfonate)-graft-poly(N,N-dimethylacrylamine) and poly(diallyldimethylammonium chloride). Core-shell assemblies of several decades of nanometers in size were revealed. The stabilization of these nanoparticles was achieved

by the nonionic grafted poly(N,N-dimethylacrylamine) side chains. In another study the formation and properties of water-soluble stoichiometric and nonstoichiometric complexes was considered.[108] PECs were assembled by cationic comb-type copolymer of the poly(acrylamide-co-[3-(methacryloylamino)propyl] trimethylammonium chloride)-graft-polyacrylamide [P(AM-co-MAPTAC)-g-PAM] with the anionic polyelectrolyte poly(sodium acrylate) (NaPA) as a function of the composition of the cationic graft copolymer in terms of PAM side chains. By increasing the number of neutral PAM side chains in the graft copolymer, the aggregation number and the size of the nanoparticles were found to decrease. Moreover, increasing the ionic strength of the solution favours the dissociation of the complexes. Larin and co-workers[106] reported on formation and properties of PECs formed by association of i) weak bottle-brush poly(acrylic acid) with oppositely charged weak linear poly(4-vinylpyridine), quaternized with ethyl bromide and ii) strong bottle brush poly([2-(methacryloyl)ethyl]-trimethylammonium iodide} with oppositely charged strong linear NaPSS in dilute aqueous solution. Regardless the strength of the ionic groups and over a wide range of complex stoichiometry, the formation of well-defined and colloidal stable nano-assemblies was demonstrated.

In a more recent study reported by the group of Muller,[109] conformational changes of a single bottle brush macromolecule was induced by oppositely charged liner polyelectrolyte. Specifically, PECs were formed by the strong cationic bottle brush copolymer poly([2-(methacryloyloxy)ethyl]trimethylammonium iodide), carrying charged side chains, with linear strong NaPSS, with two different molecular weights. Increasing the content of short NaPSS induced morphology changes of the PECs from worm-like through intermediate pearl-necklace structures to fully collapsed spheres. However, extremely long NaPSS caused the full collapse of the PECs to spheres even at very low charge ratios, without intermediate states.

In this thesis, extensive systematic research was undertaken on PECs formed by a series of bottle brush polyelectrolytes and linear polyelectrolytes. Effects of charge density, molecular weigh, concentration and charge ratio on formation, solution properties and stability of PECs is discussed in detail in Chapter 4, **Paper I-II** and **Paper V**.

2.4.7 Colloidal Stability of Polyelectrolyte Complexes

In several applications the PECs are mainly used in the form of stable homogeneous dispersions, therefore an understanding and control over the colloidal stability is of paramount importance.[110, 111] A number of suitable approaches intended to suppress PEC aggregation and to prevent precipitation have been demonstrated over the last two decades.[112, 113] Several groups have reported the stabilization of PEC micelles or nanoparticles by chemical (irreversible) cross-linking of the core or shell.[110, 114] The structure of the cross-linked micelles was fixed while their dissociation was permanently suppressed.[115] In many cases, however, these complexes have a disadvantage in terms of the biocompatibility and biodegradability of the material for medical applications. Muller et al. prepared PEC dispersions by mixing poly(diallyldimethylammonium chloride) (PDADMAC) with poly(maleic acid-co-α-methylstyrene) (PMA-MS). The PEC dispersions were stabilized by intraparticle hydrophobic interactions by phenyl residue of PMA-MS and electrostatic attraction between PMA-MS and PDADMAC and by interparticle electrostatic repulsion, respectively.[96, 97] Yet another promising strategy to overcome this problem was recently suggested, which is based on a careful design of the polyelectrolyte architecture. This approach was shown useful for achieving colloidal stability where both steric and electrostatic stabilization mechanisms can be achieved.[116, 117] Specifically, the precipiation of stoichiometric PECs can be prevented if a hydrophilic nonionic block (e.g. poly(ethylene oxide) - PEO) is attached to at least one of the polyelectrolytes.[105, 118] In such a case uncharged water-soluble PECs are formed, comprised of a water insoluble core (the insoluble PEC) surrounded and stabilized by a hydrophilic PEO corona. Such core-shell supramolecular structures are, for instance, formed by mixing poly(ethylene oxide)-*block*-poly(α,β-aspartic acid) and poly(ethylene oxide)-*block*-poly(L-lysin) diblocks, and these PECs have been shown to present chain length recognition properties.[119] The size of these assemblies was found to be in the range of some decades of nanometers. Bottle-brush polyelectrolytes, with a charged backbone and hydrophilic PEO side chains, provide an alternative strategy to prepare water-soluble stoichiometric PECs with oppositely charged linear polyelectrolytes,[106, 120, 121] as discussed in **Paper I**. Furthermore, the properties of sterically stabilized PECs, that are soluble as molecular complexes at all stoichiometries due to the presence of a high density of poly(ethylene oxide) side chains are described in **Paper II** and **Paper V**.

3. MATERIALS & EXPERIMENTAL METHODS

3.1 POLYMERS

Poly(sodium styrenesulfonate) (NaPSS) standards (M_w = 4300, 17 000, 70 000, 150 000 g mol^{-1}, M_w/M_n = 1.1) were purchased from Fluka and used as received. Copolymers of methacryloxyethyl trimethyl ammonium chloride, (METAC), and poly(ethylene oxide) methyl ether methacrylate, PEO_{45}MEMA, with three distinct molar ratios were synthesized by free-radical copolymerization at Vilnius University.[122] This results in close to random copolymers, having a M_w/M_n ratio of around 2-3, typical for polymers prepared by this method. Henceforth, PEO_{45}MEMA:METAC-X represents the general abbreviation of these brush copolymers. The subscript 45 refers to the number of ethylene oxide units in the side chains, and X denotes the molar percentage of charged units in the main chain. The molecular structures of the monomer units are schematically depicted in Figure 3.1 The short and linear polyanion, NaPSS, is composed of only one type of monomer as illustrated in Figure 3.1a. The two types of monomer units in the bottle-brush copolymers are shown in Figures 3.1b and c. Some physico-chemical characteristics of the polyelectrolytes, such as weight average molecular mass, polydispersity index determined by dynamic light scattering and number of charged units/chain are summarized in Table 3.1.

Table 3.1 Molecular characteristics of bottle brush and linear polyelectrolytes used for PEC formation.

Polyelectrolyte	*Mw* (kg mol^{-1})	M_w/M_n	*PDI*	Charged units
PEO_{45}MEMA:METAC-10	760	2-3	0.229	40
PEO_{45}MEMA:METAC-25	660	2-3	0.221	100
PEO_{45}MEMA:METAC-50	680	2-3	0.234	300
PEO_{45}MEMA:METAC-75	520	2-3	0.225	580
poly(METAC)	145	2-3	0.208	690
PSS_{4300}	4.3	1.1	-	20
PSS_{17000}	17	1.1	-	80
PSS_{70000}	70	1.1	-	340
PSS_{150000}	150	1.1	-	720

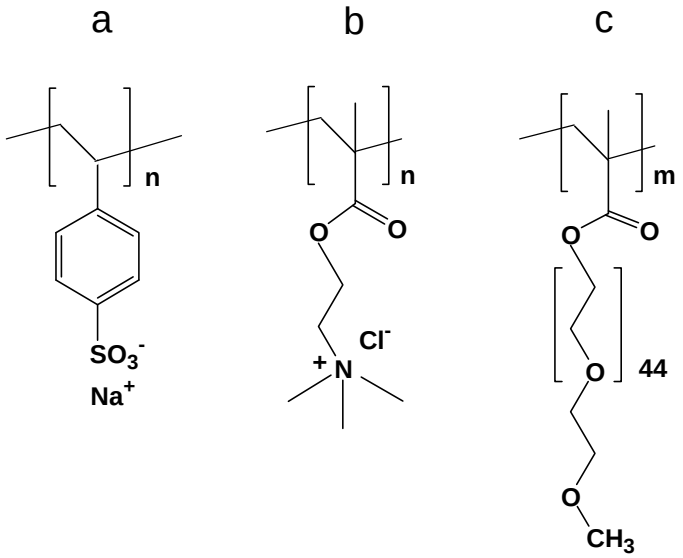

Figure 3.1 *Schematic representation of the molecular structure of the segments in the polyelectrolytes used: a) NaPSS, b) METAC, c) $PEO_{45}MEMA$.*

A homopolymer of poly(*N*-isopropylacrulamide), $PNIPAAM_{48}$, was synthesized by atom transfer radical polymerization at Oslo University following a procedure reported earlier.[123] The chemical structure of the diblock copolymers used in this study is illustrated in Figure 3.2. Poly(*N*-isopropylacrylamide)$_{48}$-block-poly((3-acrylamidopropyltrimethyl-ammonium chloride)$_X$, henceforth, $PNIPAAM_{48}$-*b*-$PAMPTMA(+)_X$, represents the general abbreviation of these block copolymers, where X represents the number of charged monomer units in the cationic block, X = 0, 6, 10, 14, 20. The polydispersity index (M_w/M_n) of the copolymers was low M_w/M = 1.05.

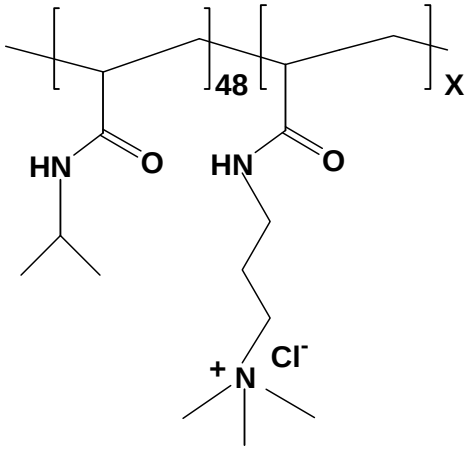

Figure 3.2 *Schematic representation of chemical structure of the cationic diblock copolymers $PNIPAAM_{48}$-b-$PAMPTMA(+)_X$. The number of charged monomer units (X) in the cationic block was X = 0, 6, 10, 14, 20.*

3.2 FORMATION OF POLYELECTROLYTE COMPLEXES

Experimental procedure. Stock solutions of the polycations with a concentration of 5000 ppm were prepared in 5 mM sodium chloride. NaPSS stock solutions were prepared in 5 mM NaCl in such a manner that the concentrations of the anionic charges from PSS were equal to the concentrations of cationic charges from the bottle-brush polyelectrolytes in their stock solutions. The PECs were formed by means of an automatic mixing process, using a programmable infusion pump (model PHD200, Harvard Apparatus, USA). Mixing was achieved by simultaneous injection of the two polyelectrolyte solutions into continuously stirred 5 mM NaCl solution. Mixtures of the following stoichiometrical ratios (5:1), (2:1), (1:1), (1:2), (1:5) between cationic groups from PEO_{45}MEMA:METAC-X and anionic groups from NaPSS were investigated.

3.3 X-RAY PHOTOELECTRON SPECTROSCOPY

The surface analytical method (XPS or ESCA) is based on the photoelectric effect.[124] In XPS experiment, a sample is exposed to monochromatic x-ray irradiation and the properties of the inner-electron shell electrons are probed.[125] If $h\nu$ is the energy of the x-ray source, and E_B is the binding energy of the electron in the atom (a function of the type of atom and its environment), the basic physics of this process can be described by the Einstein equation, simply stated: $E_B = h\nu - KE$, where KE is the kinetic energy of the emitted electron that is measured in the XPS spectrometer. The binding energy is frequently expressed in electron volts (eV). In a XPS spectrum, the electron count is plotted versus binding energy. The integrated area under the peaks in these spectra can be compared and are, after normalization with the atomic sensitivity factor, equivalent to the relative abundance of the element that is present at the surface. The analysis depth is typically 2-5 nm.

3.4 DUAL-POLARIZATION INTERFEROMETRY

Dual-polarization interferometry (DPI) is a relatively new technique, able to measure changes in thickness and refractive index of adsorbed layers *in situ* and in real time.[126] The core of the instrument is the substrate surface, which is a sandwich-like chip structure

of two horizontally stacked waveguides made of silicon oxynitride, *i.e.* nitrogen-doped silica.[127] This substrate is preferred due to its excellent optical properties with low absorption losses in the visible and near IR region combined with a high refractive index (about 1.5).[128] Silicon oxynitride has an isoelectric point at pH 3, and the zeta-potential at pH 6 is about - 50 mV as determined by streaming potential measurements.[129] When plane-polarized laser light is shone on the short end of the surface, it splits and travels separately through the two waveguides (sensing and reference). As it emerges on the other side of the chip, the two signals interfere with each other and this interference is detected by a camera as a fringe pattern in the far field. The evanescent field emitted by the sensing waveguide into the solution is affected by changes in the index of refraction and by adsorption onto the surface. Hence, the light propagating through the sensing waveguide is somewhat changed relative to the light traveling through the reference waveguide. This difference is detected as a shift in the fringe pattern in the far field, and these shifts are alternately and continuously recorded for both horizontally and vertically polarized light. By assuming formation of a homogeneous and isotropic adsorption layer, a unique solution for the thickness and refractive index of the layer can be calculated from the measured DPI signals.[130, 131]

3.5 ELECTROPHORETIC MOBILITY

A charged particle in a buffer solution is surrounded by a counterion cloud, which can be separated into two distinct regions: a thin layer tightly packed around the surface (Stern layer) that migrates with the particle in the presence of an external electric field and a more diffuse layer that migrates in the opposite direction. The surface between these two regions is defined as the surface of shear, and its electric potential is referred to as the ζ-potential. Closely related to the charge density at the particle surface, this potential controls colloidal properties such as stability and interparticle interactions. The solution electrophoretic mobility of the particle is related to the ζ-potential by the Smoluchowski relation.[132] Experimentally, the nanoparticle mobility is extracted from a measure of the inelastic frequency shift of the laser signal scattered by moving charged nanoparticles under the applied electric field.

3.6 DYNAMIC LIGHT SCATTERING

In DLS one observes the time dependent fluctuation of the scattering intensity at a given angle (q-value).[133] This process occurs due to collisions of solvent molecules with dissolved particles, known as Brownian motion, which in turn occurs due to thermal fluctuations inside the solution. These solute concentration fluctuations create short-lived domains, which vary in refractive index. The life time of these domains are related to the diffusion coefficient of the dissolved particles according to Ficks' law,[134] which in turn is related to their size.

This fluctuation of the intensity can be imagined as the drifting of particles in and out of the detection volume inside the sample cuvette. Whereas in SLS the intensity is averaged over a period of e.g. 30s, in DLS the intensity is auto-correlated with a sampling time $\Delta\tau$ down to tens of nanoseconds. The diffusion coefficient of small particles (small hydrodynamic size) is larger than that of big ones (large hydrodynamic size), and the frequency of the intensity fluctuations changes accordingly. Hence, by storing the whole intensity trace, and magnifying it, one could judge how large the particle is. However, this is not feasible due to the huge amount of produced data (using a sampling time of 30ns and 5 Byte per value one needs 166MB per second). Therefore only a correlation function g (q, τ) is computed by a commercial hardware correlator in between the output of the photo-multiplier and the computer.[135, 136] For polydisperse samples the z-average hydrodynamic size is determined.[137]

3.7 STATIC LIGHT SCATTERING

In static light scattering (SLS) the scattered intensity is collected at different angles in the horizontal x-y plane, typically between 30-150° in 5° steps. For a given angle the intensity over a period of e.g. 30s is averaged. By evaluation of the angular dependent intensity one can obtain up to three characteristics of the sample. Static light scattering data are usually analyzed in terms of the classical Zimm equation,[121] yielding the weight averaged molecular weight (M_w), the z-mean of the square of the radius of gyration ($R_{g,z}^2$), and the second virial coefficient (A_2).[138] More details on the method and instrumentation used can be found in **Papers I-II**.

4. KEY RESULTS & DISCUSSIONS

4.1 SOLUTION PROPERTIES OF BOTTLE-BRUSH POLYELECTROLYTE COMPLEXES

In this section the results from **Paper I, II, V** and additional unpublished data are the main focus. The influence of polyelectrolyte characteristics, such as charge density, molecular weigh and concentration as well as charge ratio on the formation and structural characteristics of PECs are discussed.

4.1.1 Effect of Charge Density and Concentration

Poly(METAC) / NaPSS: Stoichiometric mixing of the solutions of positively charged poly(METAC) and negatively charged NaPSS results in formation of a two phase system of supernatant liquid and precipitated PEC. Complex particles without charge excess and no steric stabilization tend toward further aggregation and in line with this phase separation was observed.[139] The preparation of non-stoichiometric complexes leads to the formation of turbid colloidal systems with suspended poly(METAC) / NaPSS particles. The solutions are turbid to the naked eye even at the lowest investigated polyelectrolyte concentration (50 ppm), in both the polycation-rich (2:1) and the polyanion-rich (1:2) cases. With increasing polyelectrolyte concentration the turbidity steeply increases and the samples become opaque. The polyanion-rich solutions (1:2) are always more turbid than the polycation rich ones (2:1) at a given concentration. This is related to the larger conversion of the polycation to PECs, which gives rise to either larger PEC concentration, or to formation of larger PEC particles or both.

The colloidal stability of the non-stoichiometric PECs was probed by repeating the turbidity measurements after storage for two weeks. The measured turbidity values were found to be identical, within the experimental error, to those measured immediately after sample preparation. Since the poly(METAC) does not contain any hydrophilic side-chains it can be concluded that the non-stochiometric complexes are stabilized electrostatically by the excess polyelectrolyte. Consistently, it was found that the complexes could be precipitated by increasing the NaCl concentration. The behavior of the nonstoichiometric and stoichiometric PEO_{45} - free system was expected and consistent

with the results of previous studies of PEC formation for analogous linear polyelectrolytes.[69]

PEO_{45}MEMA:METAC-75 / NaPSS: Mixing PEO_{45}MEMA:METAC-75 with NaPSS results in solutions that are less turbid compared to those obtained by mixing poly(METAC) and NaPSS. In the concentration range 50-200 ppm the PEO_{45}MEMA:METAC-75 / NaPSS solutions were found to be optically transparent to the naked eye, but non-zero turbidity is evident from the turbidity measurements shown in Figure 4.1a The turbidity increases linearly with polyelectrolyte concentration, which implies that the size of the formed complexes does not change significantly with polymer concentration.[140]

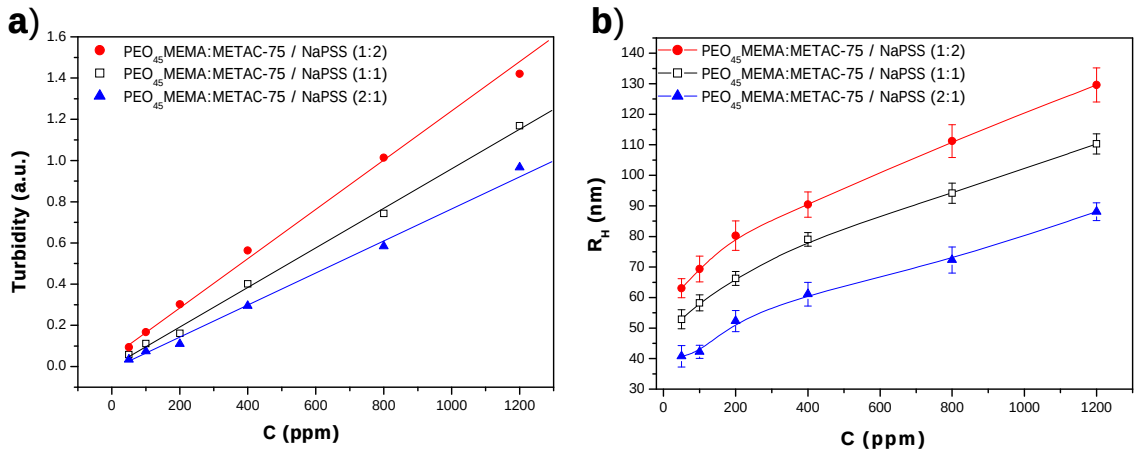

Figure 4.1 *a) Turbidity b) hydrodynamic radius vs. concentration of PEO_{45}MEMA:METAC-75 mixed with NaPSS at different mixing ratios of cationic polyelectrolyte charges to anionic polyelectrolyte charges added to the solution: (●) (1:2), (□) (1:1), and (▲) (2:1). The solid lines are plotted as guides for the eye.*

DLS measurements were also performed, and the CONTIN analysis of the measured autocorrelation functions indicated a broad, monomodal size distribution of the complexes with a polydispersity index (0.25) that was essentially the same as for the pure copolymer. This suggests that the PSS molecules are distributed uniformly among the brush polyelectrolytes. The R_H values of these PEO_{45}-poor complexes increase with polyelectrolyte concentration, as shown in Figure 4.1b. This seems to contradict to the turbidity data, which implied a constant complex size with increasing polyelectrolyte concentration. This issue can be resolved if the individual compact complexes with

increasing polyelectrolyte concentration becomes hydrodynamically coupled. In such a case the scattering intensity, and thus the turbidity, is determined by the compact core of the individual molecular complexes whereas the hydrodynamic size reflects that of the coupled cluster. For any given concentration the turbidity of the PEO_{45}-poor complexes decreases in the order of (1:2) > (1:1) > (2:1) (Figure 4.1a), and the hydrodynamic radius decreases in the same manner (Figure 4.1b). Clearly, the content of PEO_{45} side chain is not sufficient to suppress aggregation of PEO_{45}MEMA:METAC-75 / NaPSS complexes, although it prevents precipitation of stoichiometric PECs.

PEO_{45}MEMA:METAC-50 / NaPSS and PEO_{45}MEMA:METAC-25 / NaPSS: The stoichiometric (1:1) and non-stoichiometric (2:1 and 1:2) mixing of polyelectrolytes PEO_{45}MEMA:METAC-50 or PEO_{45}MEMA:METAC-25 with NaPSS leads to formation of optically transparent solutions. An increase in the polyelectrolyte concentration showed no effect on the turbidity. Further, addition of NaCl up to a concentration of 1M did not cause any increase in turbidity or precipitation. This means that the PEO_{45} side-chain content in these brush-copolymers is sufficient to achieve complete steric stabilization of the complex particles and inhibit their further aggregation.

In Figure 4.2 the hydrodynamic radius determined in aqueous 5mM NaCl solution is plotted as a function of polycation concentration for the two types of PECs formed by different mixing ratios. Clearly, R_H is concentration independent for PECs formed by both PEO_{45}MEMA:METAC-25 and PEO_{45}MEMA:METAC-50. Furthermore, the addition of NaPSS to the brush polyelectrolytes has only a minor effect on the radii of gyration as detailed in **Paper II**. The radii of gyration determined for stoichiometric PEC in presence of NaPSS (35 and 38 nm for solutions containing the 50% and 25% charge density polymers, respectively) are slightly smaller than the ones obtained for the corresponding brush polymers in absence of NaPSS. On the other hand, the scattering intensities of the solutions containing both the cationic brush polyelectrolyte and NaPSS are much larger than those of the corresponding solutions without NaPSS. Since these measurements were done at identical cationic polyelectrolyte concentrations (the small NaPSS alone does not contribute significantly to the scattering) and the radii of gyration do not change significantly upon addition of NaPSS, the increased scattering intensities must reflect an increased scattering contrast (*dn/dc*), which confirms formation of polyelectrolyte complexes.

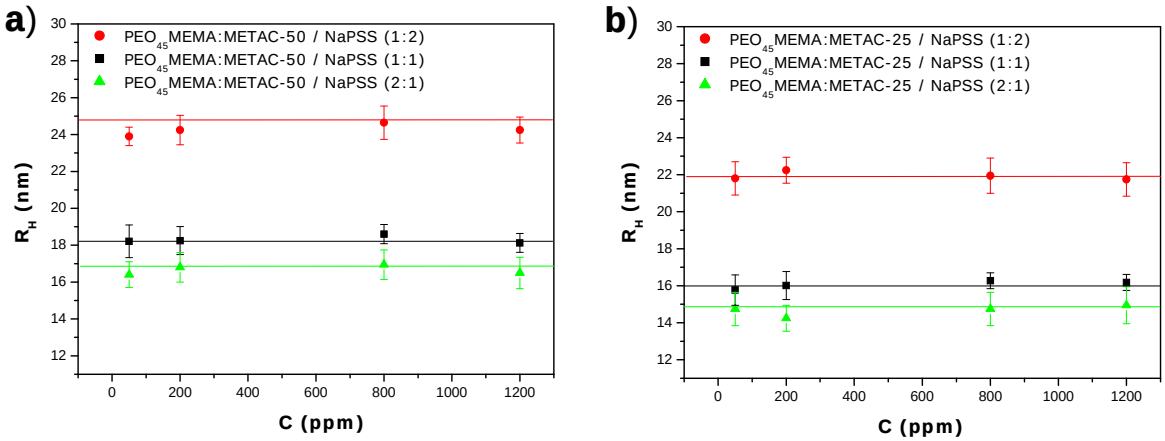

Figure 4.2 a*) Hydrodynamic radius vs. concentration of a) PEO_{45}MEMA:METAC-50 and b) PEO_{45}MEMA:METAC-25 mixed with NaPSS at different mixing ratios of cationic polyelectrolyte charges to anionic polyelectrolyte charges added to the solution: (●) (1:2), (□) (1:1), and (▲) (2:1). The solid lines are plotted as guides for the eye.*

The slight decrease of the radii of gyration on complex formation is consistent with the assumption that the NaPSS polymer is incorporated into the core of the brush, in close vicinity of the positively charged backbone. This structure can explain not only the decreasing radius of gyration but also the marginally increased hydrodynamic size (see Figure 4.2) and the increased scattering intensity that is related to the higher optical contrast of the core.

4.1.2 Effect of Polyanion Content

PEO_{45}MEMA:METAC-75 / PSS_{4300}. The hydrodynamic radius of PEO_{45}MEMA:METAC-75 / $NaPSS_{4300}$ complexes, plotted as a function of the charge fraction of NaPSS in the solution, is reported by the top curve in Figure 4.3a. An increase in NaPSS content, expressed by the ratio ([PSS]/([PSS]+[METAC])), from zero to 0.09 increased the hydrodynamic size of the PEO_{45}MEMA:METAC-75 / PSS_{4300} by a factor of 2, R_H = 42 nm, compared to the size of PEO_{45}MEMA:METAC-75 alone (20nm). Further addition of PSS up to 0.9 leads to a linear grows of R_H of the aggregates over the whole PSS range, resulting in a maximum size of the aggregates with R_H = 85 nm. Clearly, increased PSS content promotes progressive aggregation in these mixtures and the number of both small PSS and large bottle brush macromolecules incorporated in the

aggregate increases. Aggregation of PEO_{45}MEMA:METAC-75 / PSS_{4300} was also achieved by increased concentration of polyelectrolytes, as demonstrated in Section 4.1.1. The complex-aggregates were further characterized by electrophoretic mobility measurements and the results are illustrated in Figure 4.3b. Addition of the smallest amount of PSS (0.09) to PEO_{45}MEMA:METAC-75 leads to reduction of the positive mobility value of PEO_{45}MEMA:METAC-75 / $NaPSS_{4300}$, compared to the bottle brush itself. Further increasing the PSS content from 0.09 to 0.5 did not affect the mobility of the aggregates. However, when small excess of PSS is added, i.e. the PSS content is increased above 0.5, a low negative mobility of the aggregates is observed, which is not affected by further increasing the PSS content to 0.9. The low mobility values are due to the large size of the aggregates formed in this system.

PEO_{45}MEMA:METAC-50(25) / PSS_{4300}. The data-sets for hydrodynamic size obtained with these two bottle-brush polyelectrolytes of lower charge densities show the same trend. An increase in NaPSS content, from zero to 0.35 hardly affects the hydrodynamic size of the PECs, as illustrated by the bottom curves in Figure 4.3a. A further increase in PSS content results in a clear increase in the hydrodynamic radius, to a value of 23 nm for complexes with PEO_{45}MEMA:METAC-25 and to 25 nm for complexes with PEO_{45}MEMA:METAC-50. Complex formation was supported by the fact that the scattered light intensity increased for cationic PEC samples compared to the scattered intensity measured for the pure bottle-brush polyelectrolytes, and additionally by measurements of the electrophoretic mobility, summarized in Figure 4.3b. Hence, we conclude that the hydrodynamic size for both types of complexes PEO_{45}MEMA:METAC-25 / NaPSS and PEO_{45}MEMA:METAC-50 / NaPSS increases in the order (1:0) ≈ (5:1) ≈ (2:1) < (1:1) < (1:2) ≈ (1:5).

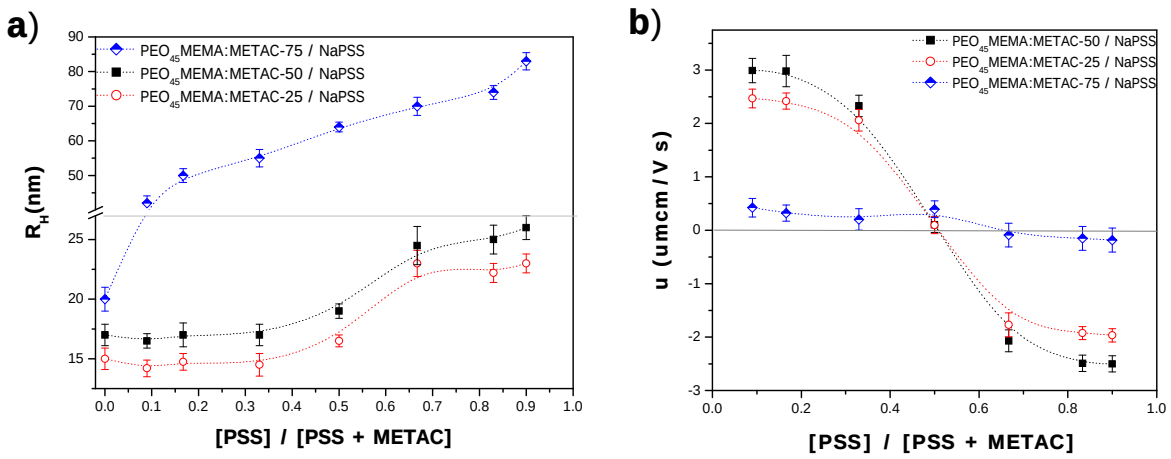

Figure 4.3 *a) Hydrodynamic radius (R_H) and b) electrophoretic mobility (u) of complexes containing PEO_{45}MEMA:METAC-50 (squares) and PEO_{45}MEMA:METAC-25 (circles) PEO_{45}MEMA:METAC-75 (half filled diamonds) as a function of the charge fraction of NaPSS. The solution contained 5 mM NaCl and 50 ppm of polyelectrolyte. Each data point represents measurements performed on separately prepared PEC samples.*

Since the hydrodynamic radius is unaffected when a small amount of PSS is incorporated in the complex, we conclude that the short and linear NaPSS present in cationic and uncharged PECs are located close to the backbone of the larger brush polyelectrolyte. In contrast, the hydrodynamic radius increases as the PECs become negatively charged, suggesting that the NaPSS chains are extended away from the backbone.

The PECs of PEO_{45}MEMA:METAC-50(25) were also characterized by electrophoretic mobility measurements, as shown in Figure 4.3b (top curves). The data for both types of PEC show the same trend. The mobility decreases as the PSS content in the solution is increased. Positive values were observed for PECs prepared in solution with excess cationic bottle-brush polymer, a close to zero mobility was found for PECs formed from stoichiometric solutions, whereas significant negative mobility values were detected for PECs prepared from solutions with excess NaPSS. These electrophoretic mobility data suggest strong complexation and formation of stoichiometric PECs when the polycation and polyanion are present in equal (charge) quantities.

4.1.3 Effect of Polyanion Molecular Weight

PEO_{45}MEMA:METAC-75/PSS_X : effect of concentration. The hydrodynamic radius of stoichiometric PEO_{45}MEMA:METAC-75/PSS_X complexes, where x = 4300, 17000,

150000 g/mol, plotted as a function of polycation concentration recorded shortly after their formation (~2 min) is shown in Figure 4.4a. Clearly, the size of the PECs increases when the polyelectrolyte concentration is increased, regardless of the molecular weight of the polyanion. The effect of concentration on the R_H suggests formation of PEC aggregates (assemblies of several polyanion - polycation macromolecules) rather than molecular complexes. At each concentration R_H decreases as the molecular weight of PSS is reduced. The hydrodynamic size was also determined for different nonstoichiometric PEO_{45}MEMA:METAC-75/PSS_X PECs. The DLS data for all nonstoichiometric compositions showed the same trend as for stoichiometric PECs, i.e. R_H increases with polyelectrolyte concentration and molecular weight of the polyanion. In addition, we found that for any given bottle-brush polyelectrolyte concentration the hydrodynamic radius of the complexes decreases in the following order (1:5) ≈ (1:2) > (1:1) > (2:1) > (5:1).

PEO_{45}MEMA:METAC-50/PSS_X and PEO_{45}MEMA:METAC-25 / PSS_X. The hydrodynamic size of the stoichiometric complexes formed by the lower charge density bottle-brush polyelectrolytes, PEO_{45}MEMA:METAC-25 and PEO_{45}MEMA:METAC-50, with different molecular weight NaPSS at different polyelectrolyte concentrations is illustrated in Figure 4.4b and c, respectively. In this case the polyelectrolyte concentration did not affect the hydrodynamic radius.

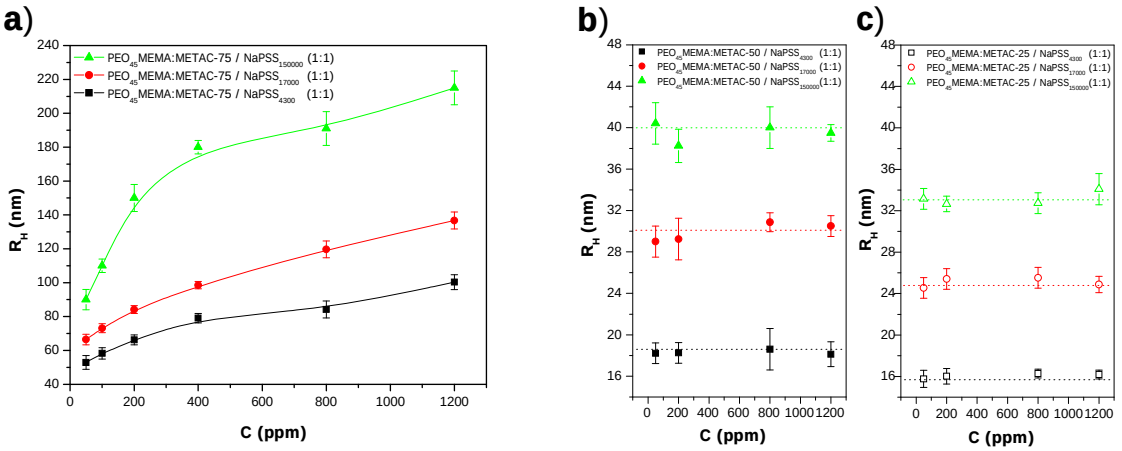

Figure 4.4 *Hydrodynamic radius of stoichiometric (1:1) complexes containing a) PEO_{45}MEMA:METAC-75 b) PEO_{45}MEMA:METAC-50 and c) PEO_{45}MEMA:METAC-25 as a function of polycation concentration. The solutions contained 5 mM NaCl. The curved lines are plotted as guides for the eye.*

Effect of PSS Molecular Weight. The hydrodynamic radius as a function of the molecular weight of NaPSS in the PECs, for different complex compositions, is reported in Figure 4.5a for PEO_{45}MEMA:METAC-50/PSS_X and in Figure 4.5b for PEO_{45}MEMA:METAC-25/PSS_X. The data-sets obtained for PECs formed with the two different bottle-brush polyelectrolytes show the same trend: increasing the molecular weight of PSS up to 70 000 g/mol leads to pronounced increase in hydrodynamic radius of the complexes, whereas a further increase in molecular weight to 150 000 g/mol hardly affects the R_H of the PECs. The size of the PEO_{45}MEMA:METAC-50 containing complexes is somewhat larger than that of the PEO_{45}MEMA:METAC-25 PECs, independently of complex stoichiometry. For both bottle-brush polyelectrolytes, at any given NaPSS molecular weight, R_H decreases as the NaPSS content is decreased, i.e. in the order (1:5) ≈ (1:2) > (1:1) > (2:1) > (5:1). Finally, it should be noted that the polydispersity index determined for PECs formed by small PSS anions (Mw ≤ 17.000 g/mol) is close to those determined for the bottle-brush polyelectrolytes, whereas larger polydispersity index is determined for the PECs containing larger molecular weight PSS (Table 4.1).

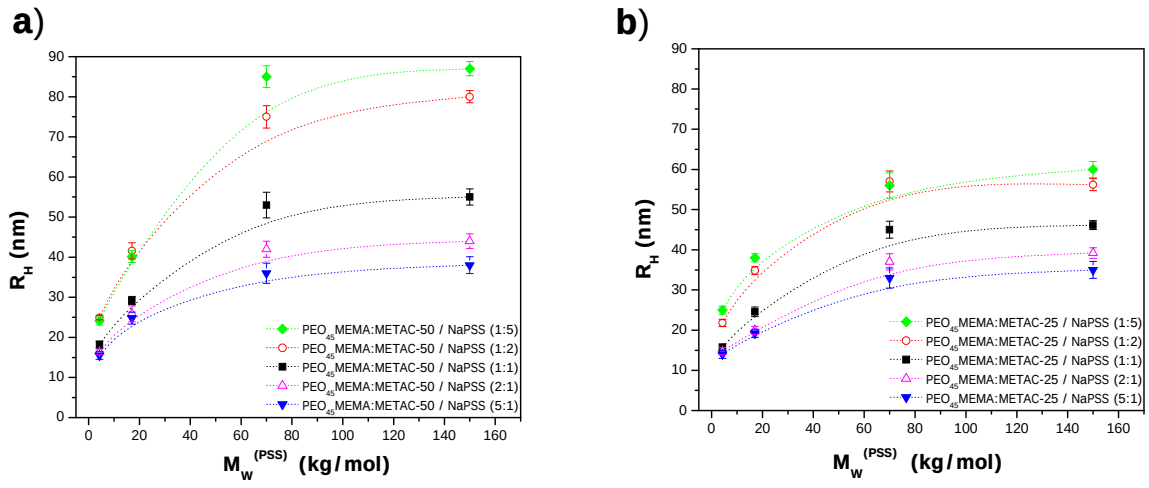

Figure 4.5 *Hydrodynamic radius of complexes containing a) PEO_{45}MEMA:METAC-50 and b) PEO_{45}MEMA:METAC-25 as a function of PSS molecular mass. The solution contained 5 mM NaCl and 50 ppm of PEO_{45}MEMA:METAC-25(50). The dashed curves are plotted as guides for the eye.*

4.1.4 Charge Characteristics of Bottle Brush Polyelectrolyte Complexes

The mean mobility values, and the standard deviation of these values from 15 experiments, for PEO_{45}MEMA:METAC-25/PSS_x and PEO_{45}MEMA:METAC-50/PSS_x complexes are plotted as a function of the ratio [PSS charges] / ([METAC charges] +

[PSS charges]) in Figure 4.6. As expected, the sign of the mobility of the PEC particles corresponds to the sign of the component in excess, and the mobility at the stoichiometric ratio (0.5) is close to zero. Regardless of the molecular weight of PSS, a further increase in PSS content results in increased negative mobility of the complexes.

The measured electrophoretic mobility, u, is influenced by the charge, Q, of the PEC particles and by their size. The number of elementary charges, z, contributing to the electrophoretic mobility of the complex can be estimated according to:

$$z = \frac{uk_BT}{eD} \tag{4.1}$$

where e is the elementary charge and D is the diffusion coefficient.

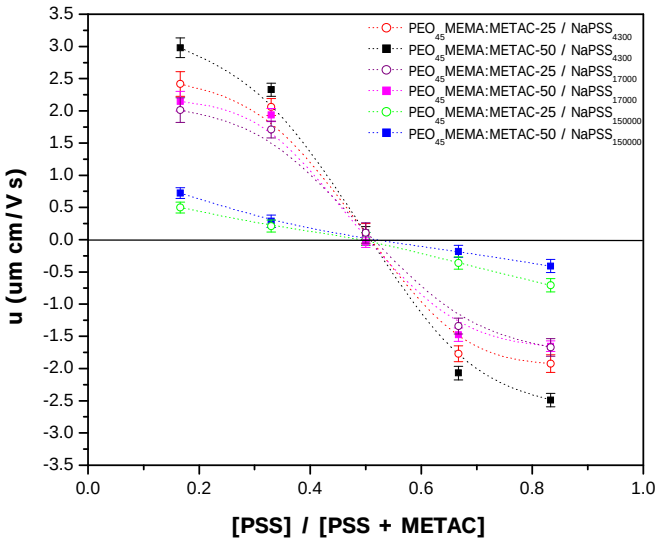

Figure 4.6 *Electrophoretic mobility vs. PSS content for (■) PEO_{45}MEMA:METAC-50/$NaPSS_X$ and (○) PEO_{45}MEMA:METAC-25/$NaPSS_X$. The concentration of the cationic polymer was fixed to 50 ppm. The horizontal line represents zero mobility. Each data point represents measurements performed on separately prepared PEC samples.*

The number of charges from small ions that are hydrodynamically associated with the PECs, z_H, can be determined using the relation $z_H = (z_{tot} - z)$, where z_{tot} is the total number of charges calculated based on the molecular composition of the polyelectrolytes.

$$z_{tot} = z_B(1-r) \tag{4.2}$$

where z_B is the charge of the bottle-brush polymer and r is the charge ratio [PSS charges]/[METAC charges] in the mixture. Numerical values for u, D, z and z_H are summarized in Table 4.1.

Table 4.1 Solution characteristics of bottle-brush polyelectrolytes and PECs.

Polyelectrolyte or PEC The PSS content is given by the ratio of PSS charges to METAC charges in the mixture	u, (10^{-8} m^2 / V·s)	D_{app} (10^{-12} m^2/s)	Z	$z_H = z_{tot}$-z	*Polydispersity index*
PEO_{45}MEMA:METAC-25	3.2	13.6	63	39	0.212
PEO_{45}MEMA:METAC-50	3.8	12.4	85	212	0.235
PEO_{45}MEMA:METAC-25/$NaPSS_{4300}$					
0.166	2.4	12.5	50	32	0.244
0.33	2.1	13.2	40	11	0.234
0.5	0.9	12.6	2	2	0.251
0.667	-1.8	9.0	-51	-2	0.235
0.833	-1.9	8.3	-60	-22	0.221
PEO_{45}MEMA:METAC-50/$NaPSS_{4300}$					
0.1666	2.9	11.2	66	172	0.225
0.33	2.3	12.2	51	97	0.236
0.5	0.1	11.1	5	5	0.242
0.667	-2.1	7.9	-67	-82	0.235
0.833	-2.5	7.5	-86	-152	0.229
PEO_{45}MEMA:METAC-25/$NaPSS_{17000}$					
0.1666	2.0	10	49	32	0.246
0.33	1.7	9.9	44	7	0.244
0.5	0.1	7.9	3	3	0.221
0.667	-1.3	5.7	-61	-10	0.245
0.833	-1.6	5.2	-80	-2	0.243
PEO_{45}MEMA:METAC-50/$NaPSS_{17000}$					
0.166	2.1	7.6	72	60	0.237
0.33	1.9	7.6	66	35	0.244
0.5	0.1	6.8	2	1	0.222
0.667	-1.5	4.8	-78	-130	0.234
0.833	-1.6	4.9	-86	-192	0.258
PEO_{45}MEMA:METAC-25/$NaPSS_{150000}$					
0.166	0.5	5.6	22	101	0.306
0.33	0.5	5.0	16	138	0.311
0.5	0.1	4.3	1	204	0.312
0.667	-0.4	3.5	-26	-127	0.359
0.833	-0.5	3.3	-42	-81	0.370
PEO_{45}MEMA:METAC-50/$NaPSS_{150000}$					
0.166	0.7	5.2	36	321	0.308
0.33	0.4	4.5	22	424	0.314
0.5	0.1	3.6	1	594	0.332
0.667	-0.2	2.5	19	-427	0.365
0.833	-0.4	2.2	46	-311	0.366

For any given charge stoichiometry of the mixture the electrophoretic mobility of the PECs decreases with the molecular weight of PSS. This is partly due to an increased size of the PEC particles, as demonstrated by dynamic light scattering measurements (see above).

Further, the absolute values for the mobility of positively and negatively charged PEO_{45}MEMA:METAC-25/PSS_x complexes were found to be somewhat lower compared to the mobility determined for PEO_{45}MEMA:METAC-50/$NaPSS_x$ PECs with the same stoichiometric ratio. This is in line with the lower number of charges in PEO_{45}MEMA:METAC-25/PSS_x complexes as compared to PEO_{45}MEMA:METAC-50/PSS_x.

The hydrodynamic charge

The average number of charges carried by the different polyelectrolytes used in this investigation is provided in Table 3.1. It should be noted that the average bottle-brush polyelectrolyte contains a larger number of charges than NaPSS of low molecular weight (4300 g/mol and 17000 g/mol), but less charges than the high molecular weight PSS (150000 g/mol). Thus, in the stoichiometric complexes several low molecular weight PSS must be associated to each bottle-brush polymer, whereas several bottle-brush polyelectrolytes must be associated to each high molecular weight PSS. It should also be noted that the polydispersity, M_w/M_n, of the polymers (Table 3.1), which is 1.1 for PSS and 2-3 for the bottle-brush polymers, obviously is important for facilitating the formation of charge stoichiometric complexes at the 1:1 mixing ratio.

The charge determined by an electrophoretic mobility measurement is equal to the charge located inside the volume defined by the liquid shear plane. Small ions are strongly accumulated close to highly charged polyelectrolytes[6] and thus the electrophoretic charge is expected to be significantly smaller than that of the polyion.[6, 8, 141] This is also observed in the data where the hydrodynamic charge of PEO_{45}MEMA:METAC-25 is about 60% of that of the polyion. The corresponding value for the more highly charged PEO_{45}MEMA:METAC-50 is about 30%. The observation that a larger fraction of the counterions resides within the hydrodynamic volume for the more highly charged bottle-brush polyelectrolyte is consistent with theoretical predictions.[142, 143] Figure 4.8 illustrates that at the stoichiometric mixing ratio the mobility is zero, and thus the number of small ions with positive charges within the hydrodynamic

volume is equal to the number of small anionic charges in the same volume. This suggests that the stoichiometry of the complex is the same as the stoichiometry of the mixture.

For the non-stoichiometric complexes, the measured charge of the PEC particles, z, is always lower in magnitude than that calculated from Eq. 4.2, z_{tot}. (Figures 4.8 a and b). For cationic complexes with low molecular weight PSS (4300 and 17000 g/mol) the net charge contribution of the hydrodynamically coupled small ions decreases as charge neutrality is approached. It is plausible to suggest that also for the cationic PECs the complex stoichiometry is the same as in the mixture. In excess of PSS we observe the expected change of sign of the complex. However, the charge of the complex is much smaller than would be expected if all PSS was incorporated in the complex, and the charge difference between the 1:2 and 1:5 complexes is small. This strongly suggests that all PSS are not incorporated in the complex but rather electrostatic repulsion between the negatively charged complex and the negative PSS puts a limit to the amount of anionic polyelectrolyte that can be incorporated. At this point the hydrodynamic volume of the complex carries an excess of about 80 negative charges.

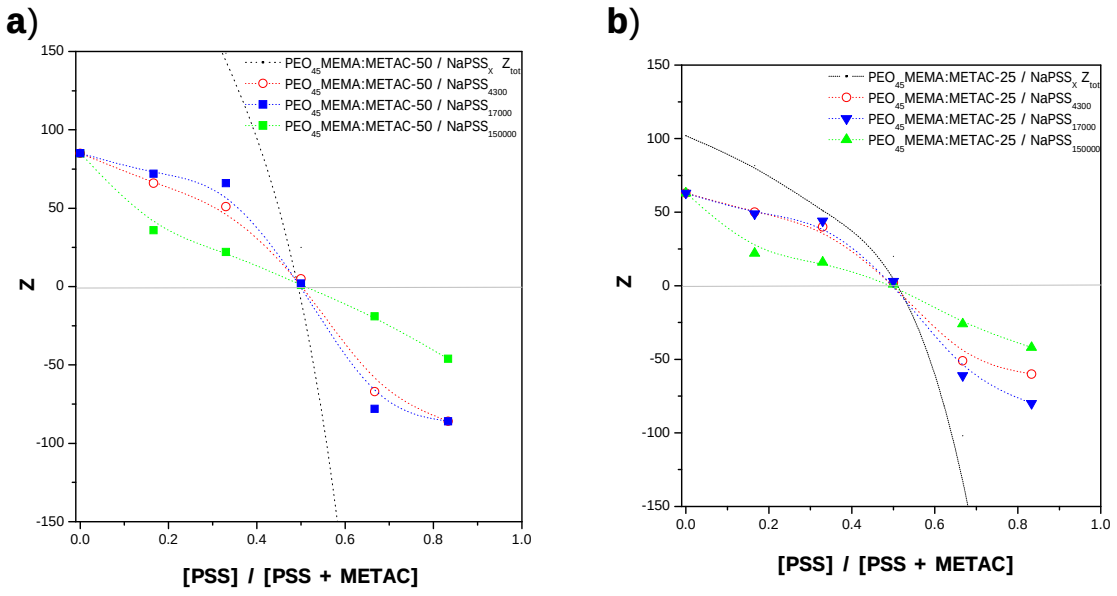

Figure 4.8 *Number of charges (Z) and total number of charges (Z_{tot}) as a function of PSS content for (a) $PEO_{45}MEMA$:METAC-50/$NaPSS_X$ and (b) $PEO_{45}MEMA$:METAC-25/$NaPSS_X$ complexes. The concentration of the cationic polymer was fixed to 50 ppm.*

The non-stoichiometric complexes formed with high molecular weight PSS have significantly lower hydrodynamic charge than those formed by low molecular weight PSS

(Figure 4.8). This is a consequence of their larger size (Figure 4.5.) that results in a larger fraction of the counterions being included in the hydrodynamic volume of the complex.

4.1.5 Structure of Bottle Brush Polyelectrolyte Complexes

The bottle-brush polymers used in this investigation has been characterized by SAXS[144] and similar bottle-brushes have also been investigated by SANS.[145] Their solution conformation can be described as being prolate with a short-axis, *b*, of about 4 nm, whereas the long-axis, *a*, is less well-defined due to the polydispersity of the polymer. The hydrodynamic radius of a prolate-shaped molecule is given by:[146]

$$R_H = \frac{Q}{\ln\left(\frac{a+Q}{b}\right)} \tag{4.3}$$

where $Q = \left(a^2 - b^2\right)^{1/2}$

By using 4 nm for the value of *b* and the measured R_H-values, the long-axis of the average bottle-brush polymer can be calculated to be about 13 nm for PEO_{45}MEMA:METAC-25 and 15 nm for PEO_{45}MEMA:METAC-50.

The cationic and stoichiometric complexes formed by PSS with molecular weight 4300 g/mol have only slightly larger hydrodynamic radius than the bottle-brush polymer alone (Figure 4.5), which suggests that the PSS is accommodated close to the backbone of the bottle-brush polymer. In contrast, the negatively charged complexes have higher R_H values. For instance, for anionic PEO_{45}MEMA:METAC-50/PSS_{4300} the R_H-value is about 25 nm compared to 17 nm for the bottle-brush alone. This change corresponds to an increase in the long and short axis of the prolate by about 1.5 nm. This increase in dimension is suggested to be partly due to stretching of the PEO side-chains due to the excluded volume repulsion exerted by the incorporated PSS, but also to the presence of some PSS molecules that extend from the bottle-brush backbone. Cationic PEO_{45}MEMA:METAC-50/PSS_{17000} PECs have similar dimension as the anionic PEO_{45}MEMA:METAC-50/PSS_{4300} PECs. This demonstrates that even the first PSS_{17000} molecules that are incorporated in the PECs partly extend from the backbone of the

bottle-brush polyelectrolyte. The anionic PECs with PSS_{17000} have a hydrodynamic radius of the order of 40 nm, which according to Eq. 4.3 means that the dimensions of the prolate have increased by about 4 nm.

The total charge of PSS_{150000} is larger than that of a typical bottle-brush polymer, and now we have the situation that several bottle-brush polymers are associated to one PSS molecule. Thus, we can no longer assume that the complex has a prolate shape. However, it is clear that the size of the complexes formed by PSS_{150000} is larger than for the PECs formed by the smaller PSS molecules (Figure 4.8), and the polydispersity of the PECs formed is also larger (Table 4.1). Just as for the complexes with low molecular weight PSS, the size of the anionic complexes is larger than that of the cationic complexes. We speculate that this is due to strong PSS-PSS repulsion within the complex resulting in a more open complex structure.

4.1.6 Colloidal Stability of Complexes

It is well known that PECs formed by linear polyelectrolytes aggregate when the electrostatic repulsion between the PECs is not sufficient to provide colloidal stability.[112, 147] The PEO_{45} side chains in the cationic bottle-brush counteract this aggregation by providing steric stabilization.

The colloidal stability of the stoichiometric and nonstoichiometric PECs in 5 mM NaCl was probed by repeating the light scattering measurements on stored samples under a period of 3 months. The hydrodynamic size of positively charged, (5:1) (2:1), and neutral (1:1) PEO_{45}MEMA:METAC-75/PSS_X (x = 4300, 17000 g/mol) complexes was found to remain constant as shown in Figure 4.9a,b for PEO_{45}MEMA:METAC-75/PSS_{4300} and in Figure 4.9c,d for PEO_{45}MEMA:METAC-75/PSS_{17000} PECs. However, the size of the negatively charged (1:5) and (1:2) nonstoichiometric PECs increased for several days due to further aggregation until precipitation occured and only small aggregates remained in solution. A similar evolution with time has been observed for mixtures of cationic polyelectrolytes mixed with anionic surfactants.[148, 149] An increase in molecular weight of the anionic polyelectrolyte to 150.000 g/mol promoted aggregation

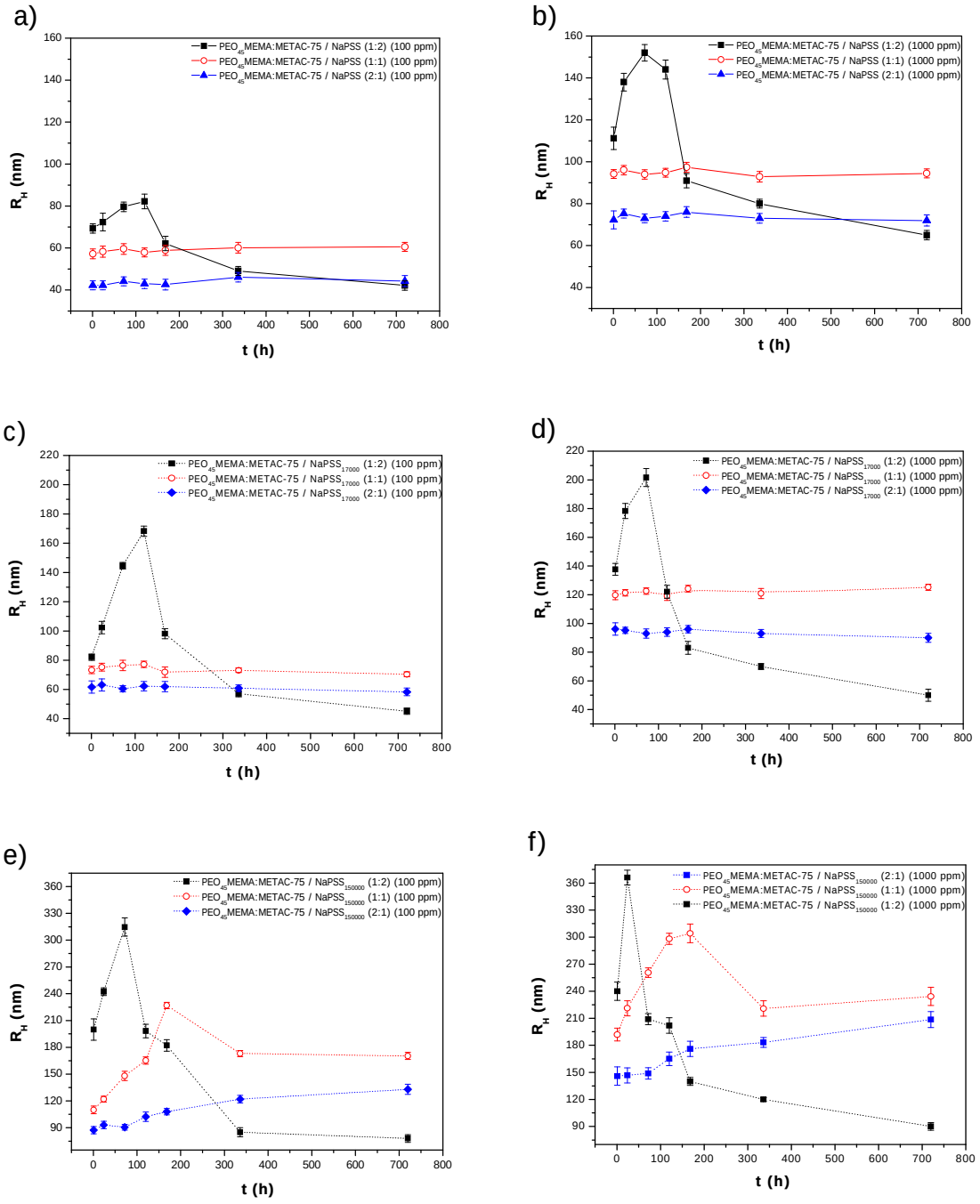

Figure 4.9 *Hydrodynamic radius (R_H) as a function of time for complexes (a,b) $PEO_{45}MEMA$:METAC-75/$NaPSS_{4300}$, (c,d) $PEO_{45}MEMA$:METAC-75/$NaPSS_{17000}$ (e,f) $PEO_{45}MEMA$:METAC-75/$NaPSS_{150000}$ at different mixing ratios of cationic polyelectrolyte charges to anionic polyelectrolyte charges added to the solution: (■) (1:2), (○) (1:1), and (▲) (2:1). The complex concentrations were (a,c,e) 100 ppm, (b,d,f) 1000 ppm. The decrease in size observed after long time for the 1:2 complexes and high molecular weigh is a result of precipitation that only leaves small aggregates in the supernatant.*

of the PEC particles, and in this case the R_H increased during several days of storage and then dropped due to sedimentation for all stoichiometries investigated, as can be seen in Figure 4.9e,f indicating limited colloidal stability regardless of the complex composition.

The hydrodynamic size of PEO_{45}MEMA:METAC-25/PSS_X and PEO_{45}MEMA:METAC- 50/PSS_X PECs, at any studied molecular weight of PSS and at any stoichiometric ratio, remained unchanged during storage for six months. This suggests formation of colloidally stable complexes. Addition of NaCl to these PEC solutions, up to a concentration of 0.5M did not cause any increase in turbidity or precipitation, which indicates that the density of uncharged PEO_{45} side-chains in the bottle-brush polymer is sufficient to achieve steric stabilization of the PECs and inhibit their further aggregation to larger particles. Clearly, the high side-chain density provides an efficient steric barrier that prevents flocculation even at high ionic strength.

4.2 ADSORPTION PROPERTIES OF BOTTLE BRUSH POLYELECTROLYTES AND POLYELECTROLYTE COMPLEXES

In this section the results from **Paper III**, **IV**, **V** and **VI** as well as additional unpublished data are the main focus. The influence of polyelectrolytes characteristics, such as charge density, molecular weigh and concentration as well as mixing (charge) ratio on adsorption properties and structural characteristics of adsorbed layers of PECs are discussed.

4.2.1 Adsorption Properties of Bottle Brush Polyelectrolytes

Adsorption properties of bottle-brush polyelectrolytes have been investigated using dual polarization interferometry (DPI). The bottle-brush copolymers PEO_{45}MEMA:METAC-X investigated have different ratios of permanent cationic charged segments and uncharged PEO side chains.

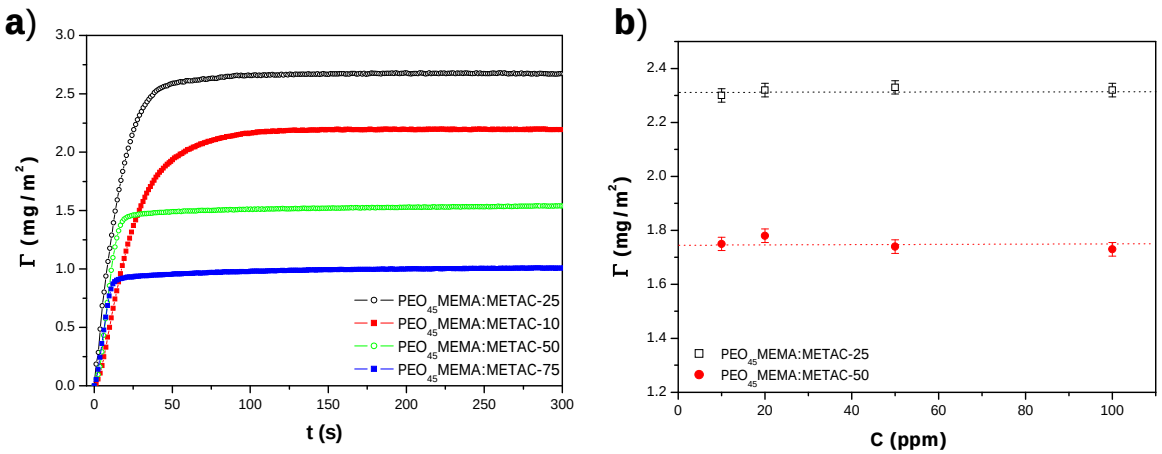

Figure 4.10 *a) Adsorbed mass as a function of time for PEO_{45}MEMA:METAC-X where X represents charge density of bottle-brush polyelectrolytes. The adsorbed layers were formed from a 100 ppm polymer solution in water. b) adsorbed mass vs. polyelectrolyte concentration for PEO_{45}MEMA:METAC-25 (open squares) and PEO_{45}MEMA:METAC-50 (closed circles) on silicon oxynitride in contact with aqueous 5 mM NaCl. The adsorption isotherms were obtained by increasing the polymer concentration stepwise.*

The adsorption on silicon oxynitride was first carried out from aqueous solution with no added inorganic salt. It was demonstrated in **Paper III** that the uncharged bottle-brush polymer, PEO_{45}MEMA, adsorbed with the backbone preferentially parallel to the surfaces to maximize the number of favorable side-chain surface interactions, whereas the

highly charged polyelectrolyte, poly(METAC), adsorbs in flat conformation, resulting in low adsorbed amounts.[150] This conformation is preferred since it leads to maximum number of electrostatic contacts with the oppositely charged silicon oxynitride surface.[151] Clearly, both the cationic groups and the PEO side chains have affinity for silicon oxynitride surfaces, and thus expected to contribute to the adsorption process of their copolymers.

The time evolution of adsorbed amount of some polymers in the PEO_{45}MEMA:METAC-X series is illustrated in Figure 4.10a. For all polymers studied the surface excess increased linearly with time during the initial stage of adsorption, and this situation prevails up to a surface coverage of 60% and 80% of the plateau value, for polymers with low (X = 10, 25) and high charge density (X = 50, 75), respectively. The maximum adsorbed amount is observed for composition X = 25. At low charge densities (10-25%) more extended layers are formed due to competition between relatively few but strong electrostatic surface polymer interaction points located at the polymer main chain, and numerous but weaker interaction points between the side chains and the surface. In contrast, at high charge densities (50-100%) electrostatic forces are predominant and relatively flat main-chain conformations on the oppositely charged surface are obtained. In this regime, when X > 50, the surface excess decreases close to linearly with increasing polyelectrolyte charge density and proceeds until (close to) charge neutrality has been reached, i.e. up to the point where the charges of the adsorbed bottle-brush polyelectrolyte compensates the surface charge.[145] Analysis of adsorbed layer thickness data detailed in **Paper III** further confirmed and complemented the above picture of the structure of the adsorbed layers of the bottle-brush copolymers.

Adsorption of bottle-brush polyelectrolytes: Effect of polyelectrolyte concentration

In **Paper IV** the adsorption of the bottle-brush polyelectrolytes PEO_{45}MEMA:METAC-25 and PEO_{45}MEMA:METAC-50 on silicon oxynitride surfaces was considered and the adsorption isotherms were obtained.[152] In this study the adsorption was performed from aqueous 5mM NaCl. For a concentration of the polyelectrolytes of 10 ppm at 20 $^{\circ}$C, adsorption equilibrium was reached within 10 min. The adsorbed amount for PEO_{45}MEMA:METAC-25 was determined to be 2.3 mg/m^2, larger than the 1.7 mg/m^2 obtained for PEO_{45}MEMA:METAC-50. The first value is slightly lower whereas the second value is slightly higher than reported above for the adsorption of these bottle-brush polyelectrolytes from water, revealed by DPI.[150] A further subsequent increase in

polyelectrolyte concentration to 20, 50, and 100 ppm did not affect the adsorbed mass as illustrated in Figure 4.10b. Hence, full coverage of the surface was reached when both polyelectrolytes were adsorbed from 10 ppm solution, indicating a high affinity to the surface. The thickness of the layers, 11.0 nm for PEO_{45}MEMA:METAC-25 and 7.3 nm for PEO_{45}MEMA:METAC-50, was also not affected by the polyelectrolyte concentration in the investigated concentration range, and slightly lower than observed in salt-free water.

4.2.2 Adsorption of Polyelectrolyte Complexes: Effect of Concentration and Polyanion Content

Effect of PEC concentration. Adsorption of PEO_{45}MEMA:METAC-25 / NaPSS and PEO_{45}MEMA:METAC-50 / NaPSS complexes with stoichiometric and non-stoichiometric compositions on silicon oxynitride surfaces was performed under identical experimental conditions as used in the adsorption experiments for the bottle-brush polyelectrolytes in **Paper IV**. As illustrated in Figure 4.11, the concentration of the PECs has no significant effect on the final adsorbed mass for any PEC composition.

Adsorption of PECs: Effect of PEC composition

Figure 4.12 clearly shows that the composition of the PECs has a pronounced effect on the adsorbed mass with cationic PECs adsorbing more than uncharged ones, and even less adsorption is achieved by the anionic PECs. This suggests that electrostatic forces are of major importance for the adsorption of these PECs to silicon oxynitride. For both stoichiometric and non-stoichiometric compositions the adsorbed amounts of the PEO_{45}MEMA:METAC-50 / $NaPSS_{4300}$ complexes were found to be lower than those obtained by the PEO_{45}MEMA:METAC-25 / $NaPSS_{4300}$ complexes.

The adsorbed amount and layer thickness as a function of the ratio [PSS]/([PSS]+[METAC]) are illustrated in Figure 4.12. For both bottle-brush polyelectrolytes we note that the adsorbed mass and the layer thickness reach a maximum at a ratio of about 0.3, corresponding to 2:1 complexes. Maximum adsorption was obtained for positively charged complexes with composition 2:1, the numerical value was found to be 2.9 mg/m^2 and the corresponding film thickness was 11.1 nm. A further increase in PSS content resulted in decreasing adsorbed mass, to about 0.2 - 0.3 mg/m^2 for anionic complexes, and layer thickness. Thus, it should be noted that anionic

complexes adsorb to some extent on the negatively charged surface. In contrast, no adsorption was detected for pure NaPSS.

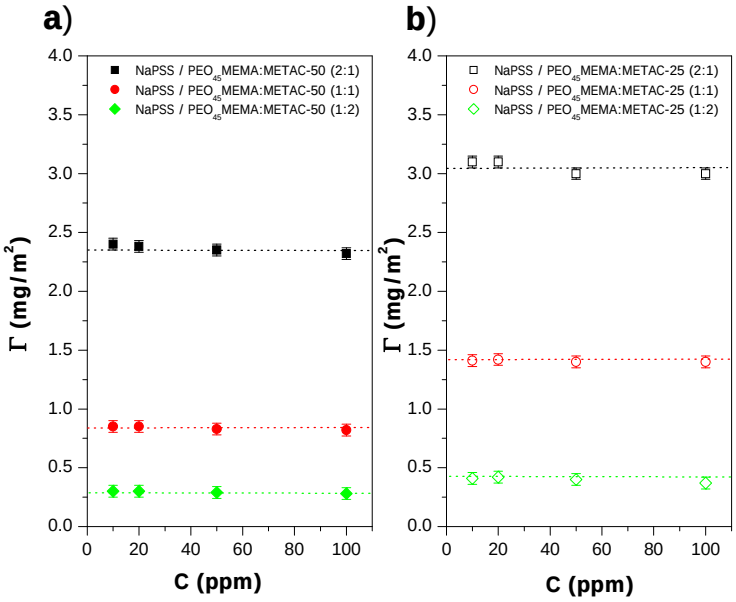

Figure 4.11 *Adsorbed mass as a function of a) PEO_{45}MEMA:METAC-50 concentration in solutions containing $NaPSS_{4300}$/ PEO_{45}MEMA:METAC-50 complexes (closed symbols) and b) PEO_{45}MEMA:METAC-25 concentration in solution containing $NaPSS_{4300}$/ PEO_{45}MEMA:METAC-25 complexes (open symbols). The adsorption isotherms were obtained by increasing the PEC concentration stepwise.*

The effect of the PSS content on the adsorption of PEO_{45}MEMA:METAC-50 / NaPSS complexes show the same general pattern as observed for the complexes formed with PEO_{45}MEMA:METAC-25 as the cationic component. However, both the adsorbed mass and thickness are significantly lower when PEO_{45}MEMA:METAC-50 is used as the cationic component as compared to when PEO_{45}MEMA:METAC-25 is employed (Figure 4.12).

Adsorption of cationic PEO_{45}MEMA:METAC-X / NaPSS complexes. The cationic complexes formed between NaPSS and the cationic bottle-brush polyelectrolytes have an electrostatic affinity for the surface. Further, the conformation of the large bottle-brush polyelectrolyte is not significantly disturbed by association with the small PSS as demonstrated by dynamic light scattering measurements. Thus, for these complexes we expect the adsorption to be driven by both electrostatic forces and the side chain - surface affinity. Thus, one reason why the adsorption increases due to addition of a small amount of NaPSS is suggested to be that larger amount of polymer is needed in order to neutralize

the surface charge density. Furthermore, the brush polymer is expected to retain some of the PSS polyions even in it surface bound state, which further increases the adsorbed amount. The fact that the XPS analysis of the surface layer demonstrates that the complex composition changes in the direction towards less PSS in the adsorbed complexes does not invalidate this explanation.

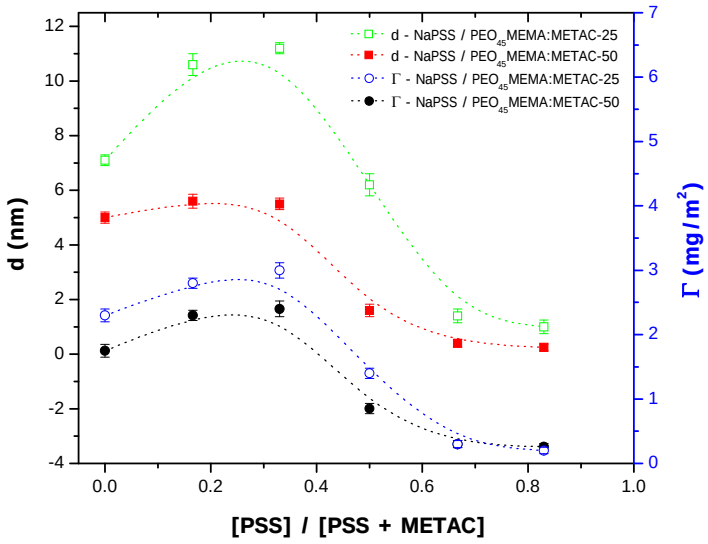

Figure 4.12 *Adsorbed mass and layer thickness as a function of PSS content in NaPSS / PEO_{45}MEMA:METAC-25 and NaPSS / PEO_{45}MEMA:METAC-50 complexes adsorbed on silicon oxynitride. Squares correspond to layer thickness, circles to adsorbed amount. Each data point was obtained from a separately prepared sample. The error bars show the standard deviation from 4 separate measurements. The concentration of the cationic polyelectrolyte was in each case 50 ppm.*

Adsorption of uncharged complexes. The uncharged poly(PEO_{45}MEMA) adsorbs significantly less than PEO_{45}MEMA:METAC-25 to silicon oxynitride (**Paper III**). The uncharged complex formed between PEO_{45}MEMA:METAC-X and NaPSS is similar to poly(PEO_{45}MEMA) in that it is a close to uncharged entity, see mobility data in Figure 4.6, with a typical bottle-brush conformation in bulk solution. Provided all PSS remained in the complex during adsorption, the complex would anyway be able to adsorb due to the affinity between the side-chains and the surface. Indeed, this seems reasonable considering that the adsorbed mass of the stoichiometric complexes, about 1 mg/m^2, is comparable to that of poly(PEO_{45}MEMA). However, the XPS results must also be considered, and they demonstrate a considerable loss of PSS from the complexes during the adsorption. Thus, the adsorption cannot be rationalized by only considering adsorption via the uncharged side chains. Rather, the XPS data suggests that the

adsorption process should be considered as being due to an ion exchange reaction, where negative surface sites and negative sites on PSS compete for binding to the positive charges on the bottle-brush polymer. Thus, the reduced adsorption for the stoichiometric complexes is primarily due to the competing binding possibility to PSS.

Adsorption of negatively charged complexes. The data illustrate that adsorption also occurs in presence of negatively charged complexes, but to a significantly smaller extent than observed for the stoichiometric complexes. This is a consequence of the increased competition from the negative charges in PSS that counteracts binding to the negative surface sites. It was shown in **Paper III** that the surface - side chain affinity is of importance during the initial adsorption of PEO_{45}MEMA:METAC-X on silicon oxynitride, and it is suggested that this is the case also for both stoichiometric and non-stoichiometric complexes. It is conceivable that the side chain affinity to the surface allows anionic complexes to reside next to the surface, despite the electrostatic repulsion. When this occurs a fraction of the small PSS molecules desorbs from the complex and this facilitates some adsorption. Due to the low adsorbed amount achieved from solutions of anionic complexes, XPS data become unreliable and thus our suggestion of desorption of PSS from anionic complexes should be viewed as a logical extrapolation of the data obtained for cationic and uncharged complexes.

4.2.3 Effect of Molecular Weight

The effect of polyanion molecular weight on adsorption properties of PEO_{45}MEMA:METAC-25(50) complexes was described in **Paper V.** The evolution of the adsorbed mass as a function of time during the initial stage of the adsorption process for PEO_{45}MEMA:METAC-25/PSS_x and PEO_{45}MEMA:METAC-50/PSS_x (x = 17.000 and 150.000 g/mol) complexes with different mixing ratios are compared in Figures 4.13a-d. From the data presented it is clear that the adsorbed amount decreases in the order (2:1) > (1:1) > (1:2), i.e. with increasing amount of anionic polyelectrolyte in the complex. Furthermore, regardless of the PEC composition, PEO_{45}MEMA:METAC-25 containing complexes adsorbed in larger amounts on silicon oxynitride compared to complexes containing the higher charge density bottle-brush polymer PEO_{45}MEMA:METAC-50.

It is also of interest to consider the initial adsorption kinetics, as evaluated from the initial slope of the curves shown in Figures 4.13a-d. Under certain assumptions (ref),[153, 154] the value of attachment rate constant k_m can, if all molecules that reach the surface adsorb, be determined from the initial slope of the adsorption curves $\left(\frac{d\Gamma}{dt}\right)_{t\to 0}$ illustrated in Figures 4.13a-d. Theoretically it is given by[155]

$$k_m = 0.98 \cdot \sqrt[3]{\frac{D_{app}^2 \cdot F}{h^2 w l}} = 12.6 \times \cdot \sqrt[3]{D_{app}^2} \qquad (4.4)$$

The prefactor in eq. 4.4 was determined for the cell used by Glaser.[156] D_{app} is the apparent diffusion constant, F the volumetric flow rate, h, w, and l are the height, width and length of the fluidic cell, respectively.

However, due to the polydispersity of the bottle-brush polyelectrolyte a direct comparison between experimental and theoretical values for k_m is difficult (see the analysis in **Paper III**). Thus, instead we take the approach to compare the variation in the measured value of k_m to the change in $D_{app}^{2/3}$ and plot the ratio $k_m / D_{app}^{2/3}$ in Figure 4.14. A constant value of this quantity means that the attachment probability is unaffected, whereas a decreased value demonstrates a decreased attachment probability. The data shown in Figures 4.14, even considering the scatter, shows that the value of $k_m / D_{app}^{2/3}$ decreases with PSS content in the PEC, and that this effect increases with increasing molecular weight of the PSS. This is not due to the increased size of the PEC, as this effect is taken into account in the factor $k_m / D_{app}^{2/3}$, but demonstrates that the adsorption probability of a PEC particle that collides with the surface decreases with PSS content and molecular weight.

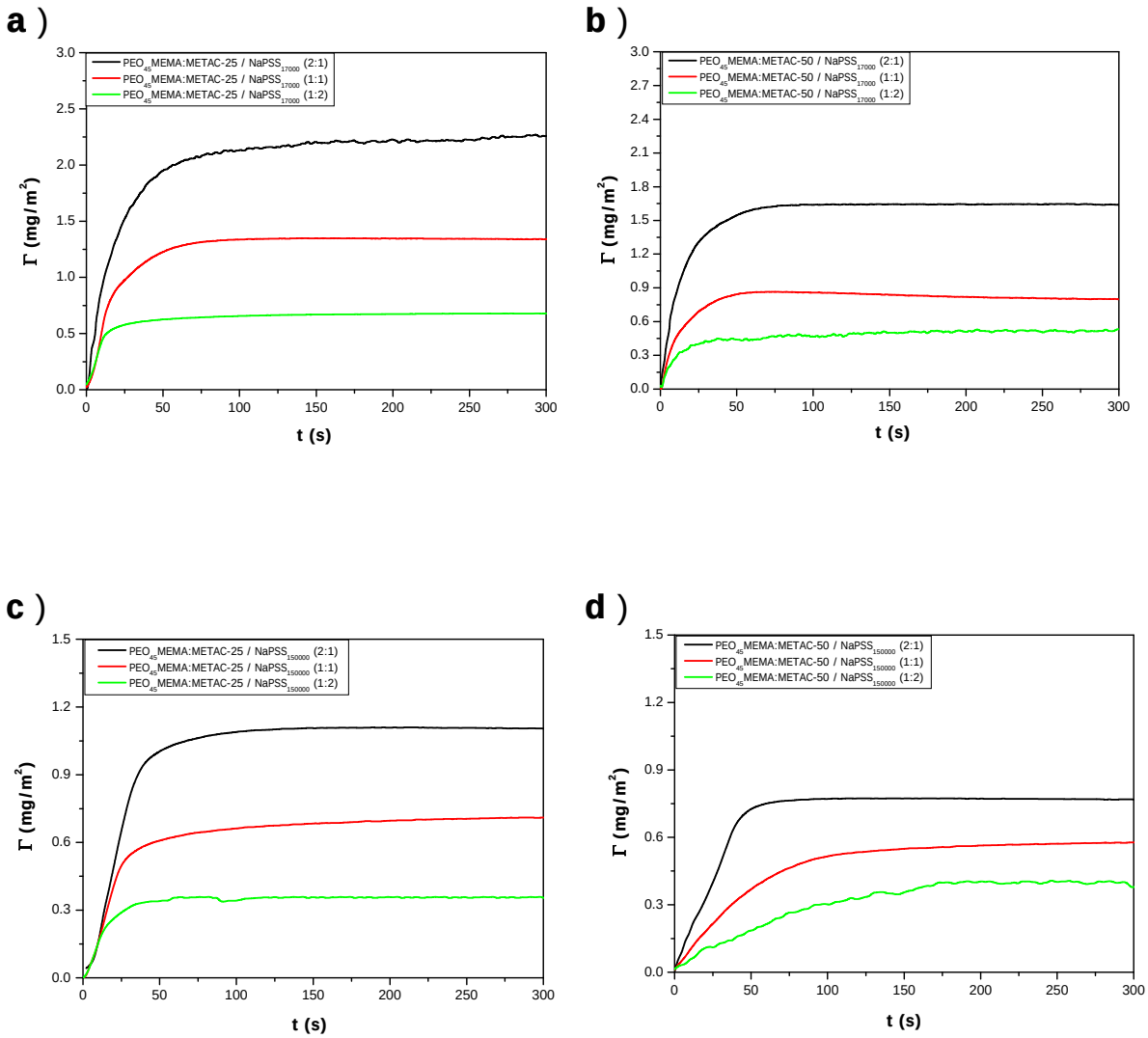

Figures 4.13 *Adsorbed mass as a function of time for a) $PEO_{45}MEMA$:METAC-25/$NaPSS_{17000}$; b) $PEO_{45}MEMA$:METAC-50/$NaPSS_{17000}$; c) $PEO_{45}MEMA$:METAC-25/$NaPSS_{150000}$ and d) $PEO_{45}MEMA$:METAC-50/$NaPSS_{150000}$ complexes on silicon oxynitride. The aqueous solution contained 5 mM NaCl.*

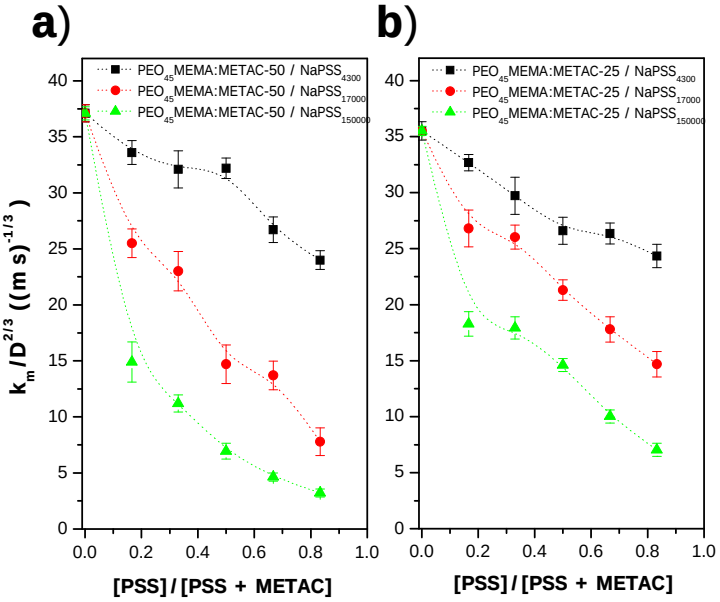

Figures 4.14 *The quantity $k_m / D_{app}^{2/3}$, where k_m is the kinetic adsorption coefficient and D the diffusion coefficient, plotted as a function of PSS charge content for a) $PEO_{45}MEMA:METAC\text{-}50/NaPSS_X$ and b) $PEO_{45}MEMA:METAC\text{-}25/NaPSS_X$ complexes containing different molecular weight PSS.*

The analysis of data for the layer thickness (**Paper 5**) showed that regardless of complex stoichiometry, the thickness of the layers formed by PEO_{45}MEMA:METAC-25 containing PECs is larger than that obtained from PECs with PEO_{45}MEMA:METAC-50. Furthermore, the thickness was found to decrease with PSS content and molecular weight.

The adsorbed amount achieved from the different PEC containing solutions are plotted as a function of NaPSS molecular weight in Figures 4.15. The data illustrate that the adsorbed mass decreases when the NaPSS molecular weight is increased. This effect is pronounced independent of the PEC composition (from 5:1 to 1:5), and in terms of absolute values the decrease is most significant for positively charged complexes.

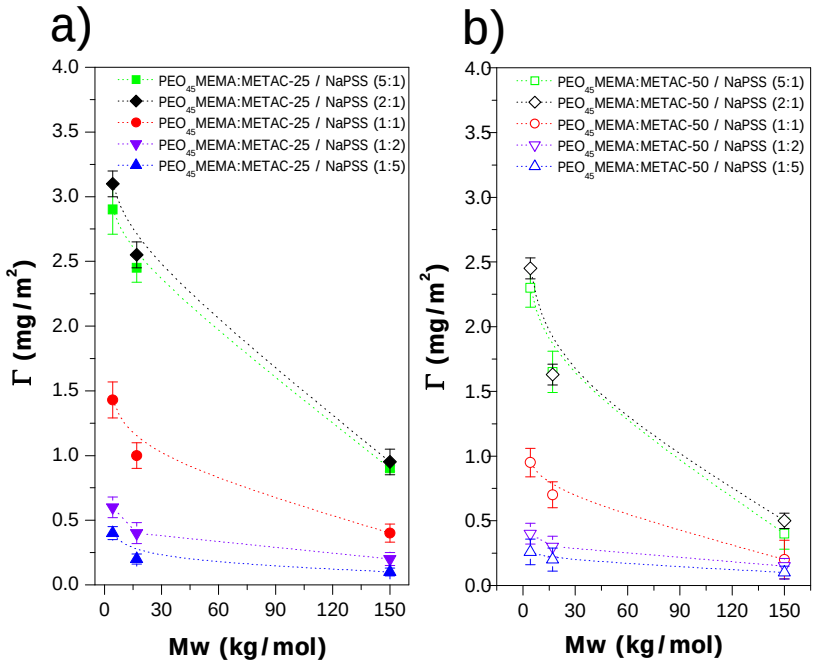

Figures 4.15 *Adsorbed mass of complexes containing a) PEO_{45}MEMA:METAC-25 and b) PEO_{45}MEMA:METAC-50 as a function of PSS molecular weight. The solution contained 5 mM NaCl and 50 ppm of PEO_{45}MEMA:METAC-25(50). The curved lines are plotted as guides for the eye.*

4.2.4 Driving Force for Adsorption

The complexes formed can in principle adsorb through electrostatic interactions with the bottle-brush backbone and through the PEO_{45} side chains, whereas the PSS molecules within the complex are repelled from the surface. Thus, when a PEC collides with the surface it can adsorb if the PEO_{45} side chains or the bottle-brush backbone encounter the surface, but not if the encounter occurs through the PSS chain. The likelihood of adsorption is thus expected to decrease with PSS content of the PEC and with increasing molecular weight of PSS since these conditions favour extended PSS chains. The plots shown in Figures 4.15 show exactly these trends.

As was discussed in chapter 4.2.2 the adsorbed layers formed by PEO_{45}MEMA:METAC-X/PSS_{4300} contain much less PSS than the complexes (**Paper IV**). In fact, so little that hardly any PSS could be detected by XPS analysis. This finding demonstrates that the low molecular weight PSS desorbs from the complex during adsorption and that adsorption proceeds through a competitive process where negative

surface sites compete with PSS for binding to the cationic sites on the bottle-brush polyelectrolyte. Provided the same mechanism prevails also for PECs formed using PSS with higher molecular weight, then one would expect the adsorbed layer to consist nearly exclusively of the bottle-brush polyelectrolyte and the layer thickness would then depend only on the adsorbed amount and not on from which PEC solution it was formed. This is indeed observed as illustrated in Figures 4.16.

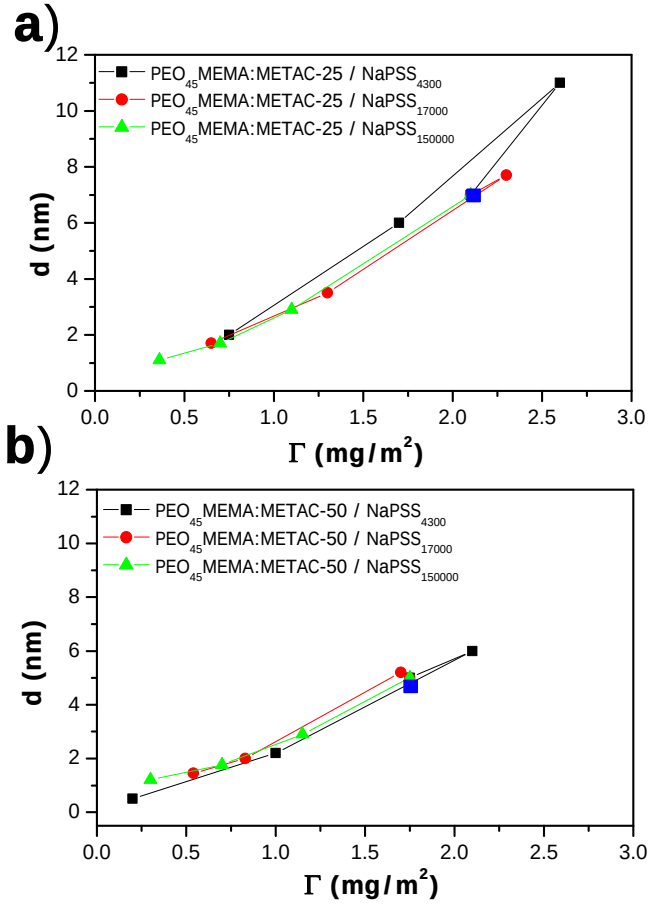

Figure 4.16 *Thickness as a function of adsorbed amount for a) PEO_{45}MEMA:METAC-25/$NaPSS_X$ b) PEO_{45}MEMA:METAC-50/$NaPSS_X$ complexes. Filled enlarged squares represent data for the bottle-brush polyelectrolyte in absence of any PSS.*

The lower adsorbed amount obtained for higher PSS content in the PEC, and for higher molecular weight of PSS for a given PSS content, is then attributed primarily to a shift in the equilibrium between surface bound and complex bound bottle-brush polymers towards the complex bound state. This is consistent with the adsorption data shown in Figure 4.13, which demonstrate that a plateau value for the adsorption is reached for each

PEC solution and thus the low adsorbed mass obtained for complexes with high PSS content is not due to slow adsorption kinetics.

4.3 ADSORPTION OF CATIONIC BLOCK COPOLYMERS

Adsorption kinetics of a series of cationic block copolymers, designated as $PNIPAAM_{48}$-*b*-$PAMPTMA(+)_X$, where (x = 0, 6, 10, 14, 20) has been investigated. The molecular structure of constituting blocks of block copolymer is depicted in Figure 3.2. Adsorption studies of highly charged polyelectrolytes with similar structure to $PAMPTMA(+)_X$ showed that polyelectrolyte adsorb in flat conformations in silica-like substrate, resulting in low adsorbed amounts and very thin adsorbed layers,[151] whereas adsorption studied of $PNIPAAM_{48}$[157] revealed affinity of this polymer to silica surface.[123]

Adsorption of a series of cationic block copolymer $PNIPAAM_{48}$-*b*-$PAMPTMA(+)_X$, where (x = 0, 6, 10, 14, 20) from water on silicon oxynitride substrates have been investigated by DPI. The time evolution of the adsorbed amount is illustrated in Figures 4.17. A common feature of all adsorption curves is that, in the initial stages of the adsorption, the adsorbed amount increases linearly with time. This is as expected for a diffusion-limited adsorption process.[158, 159]

The initial adsorption rate is similar for all of the polymers investigated, but the time required to saturate the surface is slightly larger for the copolymers, $PNIPAAM_{48}$-*b*-$PAMPTMA(+)_X$, compared to for $PNIPAAM_{48}$. This indicates that slower rearrangements in the layer occur to accommodate the last adsorbing block copolyelectrolytes. The qualitative analysis of kinetic curves, in terms of transport of molecules and their attachment rates was performed and detailed in **Paper VI**. The results showed that strong reduction in adsorption rate is due to the steric hindrance imposed by the already adsorbed polymers. In case charge reversal occurs, electrostatic interactions also slow down adsorption due to development of a depletion layer. [160]

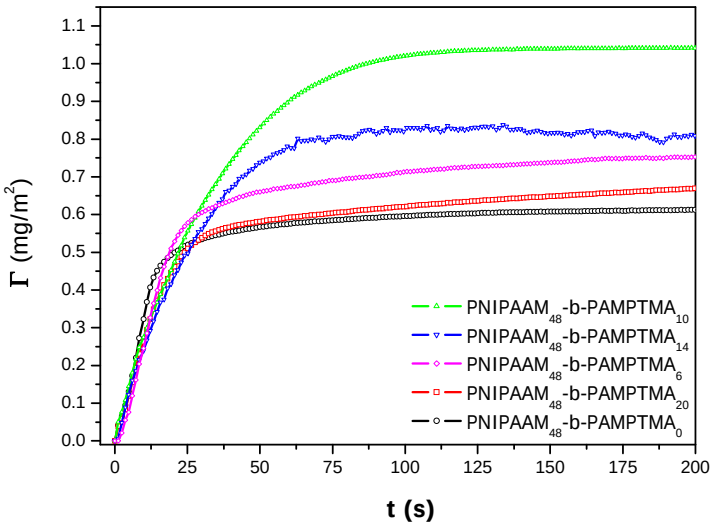

Figure 4.17 *Adsorbed mass as a function of time for PNIPAAM$_{48}$-b-PAMPTMA(+)$_X$ adsorbed from water onto silicon oxynitride. The polymer concentration was 50 ppm.*

The equilibrium adsorbed amount and thickness are shown in Figure 4.18. (Note that data for the first 200 s are shown in Figure 4.17, whereas the equilibrium adsorbed amount after about 10 min is shown in Figure 4.18). At equilibrium the adsorbed mass of PNIPAAM is 0.6 mg/m^2 and the layer thickness is 1.4 nm. This demonstrates that the PNIPAAM polymer exhibits affinity to the silicon oxynitride surface and adsorbs via non-electrostatic interactions. Incorporation of cationic block in the polymer structure increases the adsorbed amount and the maximum amount 1.1 mg/m^2 is reached when the length of the cationic block in increased to 10 units. However, a further increase in the length of the cationic block results in a decrease in adsorbed amount down to 0.7 mg/m^2 for the polymer with a 20 unit long cationic block. The variation in layer thickness mimics that of the adsorbed amount in the sense that a maximum value is found for PNIPAAM$_{48}$-*b*-PAMPTMA(+)$_{10}$. However, for a similar adsorbed mass a slightly larger thickness is observed for the cationic-rich polymers compared to the cationic-poor ones.

The adsorbed amounts in the plateau region can be recalculated in terms of number of adsorbed polymer charges and number of adsorbed polymers. The results from

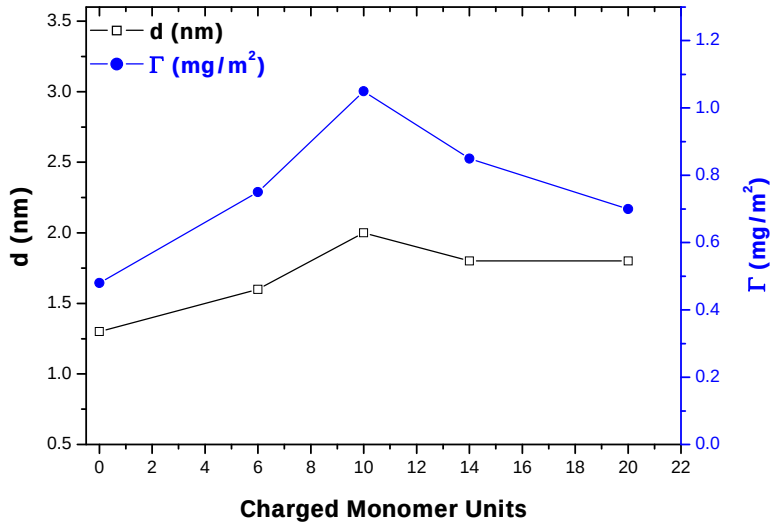

Figure 4.18 *Adsorbed mass (Γ) and thickness (d) plotted against number of charged segments in the PNIPAAM$_{48}$-b-PAMPTMA(+)$_X$ copolymer. Open squares (□) correspond to film thickness, filled circles (●) to adsorbed amount. The polymer concentration was 50 ppm and the surface was silicon oxynitride.*

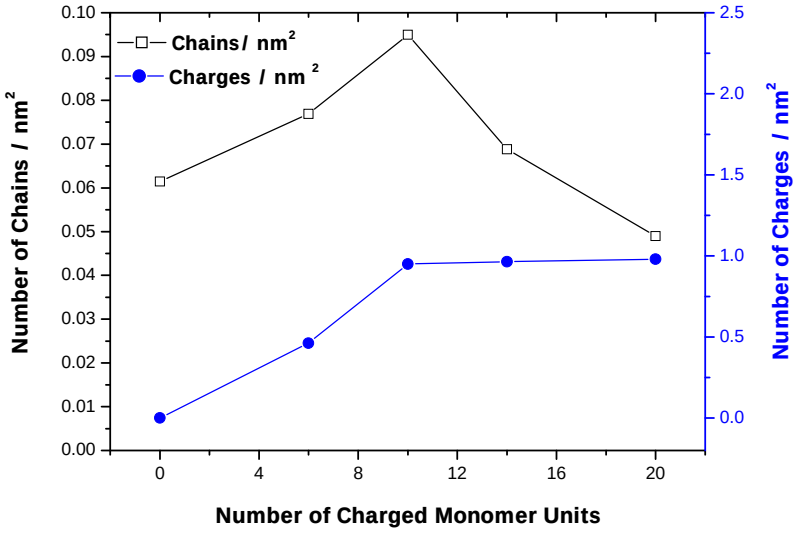

Figure 4.19 *Number of chains (□) and number of charged units (●) per nm^2 in adsorbed layers of PNIPAAM$_{48}$-b-PAMPTMA(+)$_X$ on silicon oxynitride plotted against the number of charged segments in the block copolymer.*

these calculations are shown in Figure 4.19. Interestingly, for the copolymers with 10 or more cationic groups, the same number of charged groups is adsorbed. This is a strong

indication that the adsorption is predominantly driven by electrostatic interactions and proceeds until the electrostatic repulsion between the adsorbed chains counteracts further adsorption. The number of adsorbed chains is at a maximum value for PNIPAAM$_{48}$-*b*-PAMPTMA(+)$_{10}$, whereas the number of adsorbed PNIPAAM$_{48}$-*b*-PAMPTMA(+)$_{20}$ molecules is even lower than found for PNIPAAM$_{48}$. Again, this is suggested to be a consequence of electrostatic repulsion between the adsorbed block copolyelectrolytes.

Considering the strength of electrostatic interactions it is plausible to suggest that the cationic block of the copolymer is more strongly accumulated next to the surface than the PNIPAAM block. In line with this the thickness of the adsorbed layer is dictated by the extension of the PNIPAAM block. Analysis of layer structure detailed in **Paper VI** allows one to conclude that the molecules in the adsorbed layer are in the weak overlap regime, but not stretched to such an extent that the layer can be characterized as a brush.

5. CONCLUSIONS

The thesis describes a systematic investigation of PECs formed by a series of cationic bottle-brush polyelectrolytes and a series of anionic linear polyelectrolytes in aqueous solution. Both solution and interfacial properties were considered. The pronounced effect of the side-chain density of the bottle-brush polyelectrolyte on the properties of stoichiometric and nonstoichiometric PECs was demonstrated. Formation of PECs by bottle-brush copolymers with high density of side-chains (>25%) results in small, water-soluble, molecular complexes having nonspherical shape, independent of concentration. Whereas formation of PEC-aggregates was revealed by bottle-brush polyelectrolytes with low side chain density. It was demonstrated that the morphology and the charge of the PECs can by controlled by the (charge) ratio between the polyelectrolytes. The bottle-brush polymers adopt a prolate shape in solution, and the complexation of these bottle-brushes with PSS_{4300} and PSS_{17000} leads to a moderate increase in the hydrodynamic size and no change in polydispersity, which is consistent with the picture that several small linear polyelectrolyte molecules associate with the large bottle-brush. In contrast, when complexation occurs between PSS_{150000} and the bottle-brush polymers considerably larger PECs are formed and the polydispersity increases, consistent with several bottle-brush polymers associating with one high molecular weight polyanion. In large excess of polyanion both negatively charged complexes and free polyanion molecules exist in the solution.

Adsorption kinetics of stoichiometric and nonstoichiometric PECs on negatively charged silicon oxynitride was investigated by DPI. In general, the adsorbed amount decreases with increasing PSS content of the complex, and at a given PSS content with the molecular weight of the polyanion. Further, the thickness of the layer formed scales with the adsorbed amount, and the same master curve was observed independent of PSS molecular weight. This finding is rationalized by removal of PSS from the complex during the adsorption event. The adsorbed mass achieved under a given condition is thus dictated by a competition between anionic surface sites and anionic sites on PSS for complexation with the cationic sites on the bottle-brush. This equilibrium is shifted towards the complex side with increasing PSS content and increasing PSS molecular weight. The PSS content and molecular weight also influences the initial adsorption kinetics above that expected by the different sizes of the complexes. A higher PSS

content and larger PSS molecular weight decreases the adsorption probability, which is due to the presence of extended PSS chains that counteract adsorption.

The adsorbed amount of cationic-PNIPAAM diblock copolymers was also investigated as a function of the length of the charged block. It was found that the cationic block did not significantly affect the adsorption kinetics, but it strongly affected the adsorbed mass in the plateau region. For large cationic blocks the adsorption was limited by electrostatic repulsion, whereas steric repulsion between the PNIPAAM chains limited the adsorption for short cationic blocks.

6. REFERENCES

1. Nalwa, H. S., *Handbook of Polyelectrolytes and Their Applications*. American Scientific Publishers: Stevenson Ranch, California, USA: 2002; Vol. 1-3.

2. Schmitz, K. S., *ACS Symposium Series* **1993,** *Macro-ion Characterization, Ch* 1.

3. Eisenberg, H., *Biophys. Chem.* **1977,** *7*, 3.

4. Schmitz Kenneth, S., An Overview of Polyelectrolytes. In *Macro-ion Characterization*, American Chemical Society: 1993; Vol. 548, pp 1.

5. Farinato Raymond, S., Applications of Polyelectrolytes in Aqueous Media. In *Polyelectrolytes and Polyzwitterions*, American Chemical Society: 2006; Vol. 937, pp 153.

6. Manning, G. S., *J. Chem. Phys.* **1969,** *51*, 924.

7. Manning, G. S., *The Journal of Physical Chemistry* **1981,** *85*, 1506.

8. Manning, G. S., *J. Phys. Chem. B* **2007,** *111*, 8554.

9. Flory, P., *Principles of Polymer Chemistry*. Cornell University Press: 1953.

10. De Gennes, P. G., *Scaling Concepts in Polymer Physics*. Cornell University Press: 1979.

11. Kudaibergenov, S. E.; Ciferri, A., *Macromolecular Rapid Communications* **2007,** *28*, 1969.

12. Dautzenberg, H.; Jaeger, W.; Kötz, J.; Philipp, B.; Seidel, C.; Stscherbina, D., *Polyelectrolytes: Formation, Charachterization and Application*. Hanser Publisher: Munich: 1994.

13. Dyson, R. W., *Specialty Polymers*. Second Edition ed.; Blackie Academic & Professional: 1998.

14. Enarsson, L.-E.; Wågberg, L.; Carlén, J.; Ottosson, N., *Colloids Surf., A* **2009,** *340*, 135.

15. Bolto, B.; Gregory, J., *Water Res.* **2007,** *41*, 2301.

16. Barany, S.; Szepesszentgyörgyi, A., *Adv. Colloid Interface Sci.* **2004,** *111*, 117.

17. Rojas-Reyna, R.; Schwarz, S.; Heinrich, G.; Petzold, G.; Schütze, S.; Bohrisch, J., *Carbohydrate Polymers* **2010,** *81*, 317.

18. Bijsterbosch, H. D.; Cohen Stuart, M. A.; Fleer, G. J., *J. Colloid Interface Sci.* **1999,** *210*, 37.

19. Claesson, P. M.; Dedinaite, A.; Rojas, O. J., *Adv. Colloid Interface Sci.* **2003,** *104*, 53.

20. Holmberg, K.; Jönsson, B.; Kronberg, B.; Lindman, B., *Surfactants and Polymers in Aqueous Solution*. John Willey & Sons: 2002.

21. Decher, G., *Science* **1997,** *277*, 1232–1237.

22. Park, J.; McShane, M. J., *Acs Applied Materials & Interfaces* **2010,** *2*, 991.

23. Lingström, R.; Wågberg, L., *J. Colloid Interface Sci.* **2008,** *328*, 233.

24. Darling, S. B., *Prog. Polym. Sci.* **2007,** *32*, 1152.

25. Lee, M.; Cho, B.-K.; Zin, W.-C., *Chemical Reviews* **2001,** *101*, 3869.

26. Riess, G., *Prog. Polym. Sci.* **2003,** *28*, 1107.

27. Hayward, R. C.; Pochan, D. J., *Macromolecules* **2010,** *43*, 3577.

28. Astafieva, I.; Zhong, X. F.; Eisenberg, A., *Macromolecules* **1993,** *26*, 7339.

29. Nakashima, K.; Bahadur, P., *Adv. Colloid Interface Sci.* **2006,** *123-126*, 75.

30. O'Reilly, R. K.; Hawker, C. J.; Wooley, K. L., *Chemical Society Reviews* **2006,** *35*, 1068.

31. Martien A. Cohen Stuart, W. T. S. H., Jan Genzer, Marcus Müller, Christopher Ober, Manfred Stamm, Gleb B. Sukhorukov, Igal Szleifer, Vladimir V. Tsukruk, Marek Urban, et al., *Nature Materials* **2010,** *9*, 101.

32. Schumers, J. M.; Fustin, C. A.; Gohy, J. F., *Macromolecular Rapid Communications* **2010,** *31*, 1588.

33. Shim, W. S.; Yoo, J. S.; Bae, Y. H.; Lee, D. S., *Biomacromolecules* **2005,** *6*, 2930.

34. Motornov, M.; Sheparovych, R.; Lupitskyy, R.; MacWilliams, E.; Minko, S., *J. Colloid Interface Sci.* **2007,** *310*, 481.

35. Dimitrov, I.; Trzebicka, B.; Müller, A. H. E.; Dworak, A.; Tsvetanov, C. B., *Prog. Polym. Sci.* **2007,** *32*, 1275.

36. Rodríguez-Hernández, J.; Chécot, F.; Gnanou, Y.; Lecommandoux, S., *Prog. Polym. Sci.* **2005,** *30*, 691.

37. Motornov, M.; Roiter, Y.; Tokarev, I.; Minko, S., *Prog. Polym. Sci.* **2010,** *35*, 174.

38. Andre, X.; Zhang, M. F.; Muller, A. H. E., *Macromolecular Rapid Communications* **2005,** *26*, 558.

39. Bütün, V.; Liu, S.; Weaver, J. V. M.; Bories-Azeau, X.; Cai, Y.; Armes, S. P., *Reactive and Functional Polymers* **2006,** *66*, 157.

40. Oh, K. T.; Bronich, T. K.; Bromberg, L.; Hatton, T. A.; Kabanov, A. V., *Journal of Controlled Release* **2006,** *115*, 9.

41. Gilmore, J. L.; Yi, X.; Quan, L.; Kabanov, A. V., *Journal Of Neuroimmune Pharmacology* **2008,** *3*, 83.

42. Kabanov, A. V.; Kabanov, V. A., *Advanced Drug Delivery Reviews* **1998,** *30*, 49.

43. Elabd, Y. A.; Hickner, M. A., *Macromolecules* **2011,** *44*, 1.

44. Savage, N.; Diallo, M. S., *Journal Of Nanoparticle Research* **2005,** *7*, 331.

45. Perelstein, O. E.; Ivanov, V. A.; MoÌˆller, M.; Potemkin, I. I., *Macromolecules* **2010,** *43*, 5442.

46. Leea, H.-i.; Pietrasik, J.; Sheiko, S. S.; Matyjaszewski, K., *Prog. Polym. Sci.* **2010,** *35*, 24.

47. Mori, H.; Müller, A. H. E., *Prog. Polym. Sci.* **2003,** *28*, 1403.

48. Zhang, B.; GrÃ¶hn, F.; Pedersen, J. S.; Fischer, K.; Schmidt, M., *Macromolecules* **2006,** *39*, 8440.

49. Panyukov, S.; Zhulina, E. B.; Sheiko, S. S.; Randall, G. C.; Brock, J.; Rubinstein, M., *J. Phys. Chem. B* **2009,** *113*, 3750.

50. Wintermantel, M.; Gerle, M.; Fischer, K.; Schmidt, M.; Wataoka, I.; Urakawa, H.; Kajiwara, K.; Tsukahara, Y., *Macromolecules* **1996,** *29*, 978.

51. Matyjaszewski, K.; Xia, J., *Chemical Reviews* **2001,** *101*, 2921.

52. Pietrasik, J.; Tsarevsky, N. V., *European Polymer Journal* **2010,** *46*, 2333.

53. Tsarevsky, N. V.; Matyjaszewski, K., *Chemical Reviews* **2007,** *107*, 2270.

54. Feng, C.; Li, Y.; Yang, D.; Hu, J.; Zhang, X.; Huang, X., *Chemical Society Reviews* **2009,** *40*, 1282.

55. Jaeger, W.; Bohrisch, J.; Laschewsky, A., *Prog. Polym. Sci.* **2010,** *35*, 511.

56. Waigh, T. A.; Papagiannopoulos, A., *Polymers* **2010,** *2*, 57.

57. Seyrek, E.; Dubin, P., *Adv. Colloid Interface Sci.* **2010,** *158*, 119.

58. Stevenson, W.; Chang, R.; Gebremichael, Y., *J. Mol. Biol.* **2011,** *405*, 1101.

59. Han, L.; Dean, D.; Ortiz, C.; Grodzinsky, A. J., *Biophys. J.* **2007,** *92*, 1384.

60. Svensson, O.; Arnebrant, T., *Curr. Opin. Colloid Interface Sci.* **2010,** *In Press, Corrected Proof*.

61. Dedinaite, A., *Encyclopedia of Surface and Colloid Science* **2010**.

62. Moghimi, S. M.; Hunter, A. C.; Murray, J. C., *Faseb Journal* **2005,** *19*, 311.

63. Philipp, B.; Dautzenberg, H.; Linow, K.-J.; Kotz, J.; Dawydoff, W., *Prog. Polym. Sci.* **1989,** *14*, 91.

64. Fuoss, R. M.; Sadek, H., *Science* **1949,** *110*, 552.

65. Michaels, A. S.; Miekka, R. G., *J. Phys. Chem.* **1961,** *65*, 1765.

66. Nylander, T.; Samoshina, Y.; Lindman, B., *Adv. Colloid Interface Sci.* **2006,** *123-126*, 105.

67. Vanerek, A.; van de Ven, T. G. M., *Colloids And Surfaces A-Physicochemical And Engineering Aspects* **2006,** *273*, 55.

68. Kabanov, A. V.; Kabanov, V. A., *Bioconjug. Chem.* **1995,** *6*, 7.

69. Kabanov, V. A., *Usp. Khim.* **2005,** *74*, 5.

70. Bucur, C. B.; Sui, Z.; Schlenoff, J. B., *J. Am. Chem. Soc.* **2006,** *128*, 13690.

71. Zhaoyang, O.; Muthukumar, M., *J. Chem. Phys.* **2006,** *124*, 154902.

72. Michaels, A. S., *Ind. Eng. Chem.* **1965,** *57*, 32.

73. Hartig, S. M.; Greene, R. R.; Dikov, M. M.; Prokop, A.; Davidson, J. M., *Pharm. Res.* **2007,** *24*, 2352.

74. Thunemann, A. F.; Muller, M.; Dautzenberg, H.; Joanny, J. F. O.; Lowne, H., Polyelectrolyte complexes. In *Polyelectrolytes With Defined Molecular Architecture II*, 2004; Vol. 166, pp 113.

75. Ankerfors, C.; Ondaral, S.; Wågberg, L.; Ödberg, L., *J. Colloid Interface Sci.* **2010,** *351*, 88.

76. Michaels, A. S.; Mir, L.; Schneider, N. S., *J. Phys. Chem.* **1965,** *69*, 1447.

77. Tsuchida, E.; Osada, Y.; Sanada, K., *J. Polym. Sci., Part A: Polym. Chem.* **1972,** *10*, 3397.

78. Starodubtsev, S. G.; Kabanov, V. A., *Polymer Science U.S.S.R.* **1977,** *19*, 2229.

79. Kharenko, O. A.; Izumrudov, V. A.; Kharenko, A. V.; Kasaikin, V. A.; Zezin, A. B.; Kabanov, V. A., *Vysokomolekulyarnye Soedineniya Seriya A* **1980,** *22*, 218.

80. Bakeev, K. N.; Izumrudov, V. A.; Kuchanov, S. I.; Zezin, A. B.; Kabanov, V. A., *Macromolecules* **1992,** *25*, 4249.

81. Pergushov, D. V.; Izumrudov, V. A.; Zezin, A. B.; Kabanov, V. A., *Vysokomolekulyarnye Soedineniya Seriya A & Seriya B* **1993,** *35*, A844.

82. Tsuchida, E., *J. Macromol. Sci., Chem.* **1994,** *A31*, 1.

83. Zintchenko, A.; Dautzenberg, H.; Tauer, K.; Khrenov, V., *Langmuir* **2002,** *18*, 1386.

84. Zintchenko, A.; Rother, G.; Dautzenberg, H., *Langmuir* **2003,** *19*, 2507.

85. Dautzenberg, H., *Macromolecules* **1997,** *30*, 7810.

86. Dautzenberg, H.; Gao, Y.; Hahn, M., *Langmuir* **2000,** *16*, 9070.

87. Dautzenberg, H.; Kriz, J., *Langmuir* **2003,** *19*, 5204.

88. Kramarenko, E. Y.; Khokhlov, A. R.; Reineker, P., *J. Chem. Phys.* **2006,** *125*.

89. Kramarenko, E. Y.; Pevnaya, O. S.; Khokhlov, A. R., *J. Chem. Phys.* **2005,** *122*.

90. Krotova, M. K.; Vasilevskaya, V. V.; Leclercq, L.; Boustta, M.; Vert, M.; Khokhlov, A. R., *Macromolecules* **2009,** *42*, 7495.

91. Vasilevskaya, V. V.; Leclercq, L.; Boustta, M.; Vert, M.; Khokhlov, A. R., *Macromolecules* **2007,** *40*, 5934.

92. Hayashi, Y.; Ullner, M.; Linse, P., *J. Phys. Chem. B* **2004,** *108*, 15266.

93. Carlsson, F.; Linse, P.; Malmsten, M., *J. Phys. Chem. B* **2001,** *105*, 9040.

94. KUROKAWA, Y.; SHIRAKAWA, N.; TERADA, M.; YUI, N., *Journal of Applied Polymer Science* **1980,** *25*, 1645.

95. Vasheghani, B. F.; Rajabi, F. H.; Ahmadi, M. H.; Mashhadi, F., *Polymer Bulletin* **2008,** *61*, 247.

96. Reihs, T.; Müller, M.; Lunkwitz, K., *J. Colloid Interface Sci.* **2004,** *271*, 69.

97. Muller, M.; Kessler, B.; Richter, S., *Langmuir* **2005,** *21*, 7044.

98. Reihs, T.; Müller, M.; Lunkwitz, K., *Colloids Surf., A* **2003,** *212*, 79.

99. Pergushov, D. V.; Babin, I. A.; Plamper, F. A.; Zezin, A. B.; Muller, A. H. E., **2008,** *24*, 6114.

100. Zhang, H.; Dubin, P. L.; Ray, J.; Manning, G. S.; Moorefield, C. N.; Newkome, G. R., *J. Phys. Chem. B* **1999,** *103*, 2347.

101. Miura, N.; Dubin, P. L.; Moorefield, C. N.; Newkome, G. R., *Langmuir* **1999,** *15*, 4245.

102. Larin, S. V.; Darinskii, A. A.; Zhulina, E. B.; Borisov, O. V., *Langmuir* **2009,** *25*, 1915.

103. Grohn, F., *Macromolecular Chemistry And Physics* **2008,** *209*, 2295.

104. Matralis, A.; Sotiropoulou, M.; Bokias, G.; Staikos, G., *Macromolecular Chemistry and Physics* **2006,** *207*, 1018.

105. Sotiropoulou, M.; Bokias, G.; Staikos, G., *Biomacromolecules* **2005,** *6*, 1835.

106. Larin, S. V.; Pergushov, D. V.; Xu, Y.; Darinskii, A. A.; Zezin, A. B.; Muller, A. H. E.; Borisov, O. V., *Soft Matter* **2009,** *5*, 4938.

107. Sotiropoulou, M.; Bossard, F.; Balnois, E.; Oberdisse, J.; Staikos, G., *Langmuir* **2007,** *23*, 11252.

108. Sotiropoulou, M.; Cincu, C.; Bokias, G.; G, S., *Polymer* **2004,** *45*, 1563.

109. Xu, Y.; Borisov, O. V.; Ballauff, M.; Muller, A. H. E., *Langmuir* **2010,** *26*, 6919.

110. Akagi, T.; Watanabe, K.; Kim, H.; Akashi, M., *Langmuir* **2009,** *26*, 2406.

111. Mani, E.; Sanz, E.; Bolhuis, P. G.; Kegel, W. K., *The Journal of Physical Chemistry C* **2010,** *114*, 7780.

112. Mihai, M.; Dragan, E. S.; Schwarz, S.; Janke, A., *J. Phys. Chem. B* **2007,** *111*, 8668.

113. Dragan, E. S.; Mihai, M.; Schwarz, S., *Colloids And Surfaces A-Physicochemical And Engineering Aspects* **2006,** *290*, 213.

114. Hu, Y. C., Y.; Chen, Q.; Zhang, L.; Jiang, X.; Yang, C, *Polymer* **2005,** *46*, 12703–12710.

115. Zhang, J. Z., Y.; Zhu, Z.; Ge, Z.; Liu, S, *Macromolecules* **2008,** *41*, 1444–1454.

116. Naderi, A.; Iruthayaraj, J.; Pettersson, T.; x; rn; Makus; x30c; ka, R.; x30c; ardas; Claesson, P. M., *Langmuir* **2008,** *24*, 6676.

117. Naderi, A.; Iruthayaraj, J.; Vareikis, A.; Makuska, R.; Claesson, P. M., *Langmuir* **2007,** *23*, 12222.

118. Cohen Stuart, M. A.; Hofs, B.; Voets, I. K.; de Keizer, A., *Curr. Opin. Colloid Interface Sci.* **2005,** *10*, 30.

119. Harada, A.; Kataoka, K., *Science* **1999,** *283*, 65.

120. Shovsky, A. V.; Varga, I.; Makuska, R.; Claesson, P. M., *J. Dispersion Sci. Technol.* **2009,** *30*, 980.

121. Shovsky, A.; Varga, I.; Makuska, R.; Claesson, P. M., *Langmuir* **2009,** *25*, 6113.

122. Iruthayaraj, J.; Poptoshev, E.; Vareikis, A.; Makuska, R.; van der Wal, A.; Claesson, P. M., *Macromolecules* **2005,** *38*, 6152.

123. Dedinaite, A.; Thormann, E.; Olanya, G.; Claesson, P. M.; Nystrom, B.; Kjoniksen, A. L.; Zhu, K. Z., *Soft Matter* **2010,** *6*, 2489.

124. Ulman, A.; Elman, J. F., *Characterization of organic thin films*. Butterworth-Heinemann: Greenwich, 1995.

125. Andrade, J. D., *Surface and Interfacial Aspects Biomedical Polymers*. Plenum: New York, 1985.

126. Cross, G. H.; Reeves, A. A.; Brand, S.; Popplewell, J. F.; Peel, L. L.; Swann, M. J.; Freeman, N. J., *Biosensors and Bioelectronics* **2003,** *19*, 383.

127. Germann, R.; Salemink, H. W. M.; Beyeler, R.; Bona, G. L.; Horst, F.; Massarek, I.; Offrein, B. J., *Journal of The Electrochemical Society* **2000,** *147*, 2237.

128. Worhoff, K.; Lambeck, P. V.; Driessen, A.; Member, S., *J. Lightwave Technol.* **1999,** *17*, 1401.

129. Krivocheeva, O.; Dedinaite, A.; Claesson, P. M., **2011**.

130. Cross, G. H.; Reeves, A.; Brand, S.; Swann, M. J.; Peel, L. L.; Freeman, N. J.; Lu, J. R., *J. Phys. D: Appl. Phys.* **2004,** *37*, 74.

131. Freeman, N. J.; Peel, L. L.; Swann, A. M. J.; Reeves, G. H. C. A.; Brand, S.; Lu, J. R., *Journal of Physics: Condensed Matter* **2004**, S2493.

132. Hoagland, D. A.; Arvanitidou, E.; Welch, C., *Macromolecules* **1999,** *32*, 6180.

133. Schmitz, K. S., *An introduction to Dynamic Light Scattering by Macromolecules*. Academic Press Limited: London, 1990.

134. Brown, W., *Light Scattering Principles and Development*. Clarendon Press, Oxford: 1996.

135. Brown, J. C.; Pusey, P. N.; Goodwin, J. W.; Ottewill, R. H., *Journal Of Physics A: Mathematical And General* **1975,** *8*, 664.

136. Brown, J. C.; Pusey, P. N., *J. Phys. D: Appl. Phys.* **1974,** *7*, L31.

137. Degiorgio, V.; Piazza, R., *Curr. Opin. Colloid Interface Sci.* **1996,** *1*, 11.

138. Gun'ko, V. M.; Klyueva, A. V.; Levchuk, Y. N.; Leboda, R., *Adv. Colloid Interface Sci.* **2003,** *105*, 201.

139. Doi, R.; Kokufuta, E., *Langmuir* **2011,** *26*, 13579.

140. Dautzenberg, H.; Rother, G.; Hartmann, J., Light-Scattering Studies of Polyelectrolyte Complex Formation. In *Macro-ion Characterization*, American Chemical Society: 1993; Vol. 548, pp 210.

141. Manning, G. S., *J. Phys. Chem. B* **2010,** *114*, 5435.

142. Dobrynin, A. V.; Rubinstein, M., *Prog. Polym. Sci.* **2005,** *30*, 1049.

143. Dobrynin, A. V., *Curr. Opin. Colloid Interface Sci.* **2008,** *13*, 376.

144. Dedinaite, A.; Bastardo, L.; Oliveira, C. P.; Pedersen, J. S.; Claesson, P. M.; Vareikis, A.; Makuska, R., *Proceed. Baltic Polymer Symposium* **2007**, 112.

145. Bastardo, L. A.; Iruthayaraj, J.; Lundin, M.; Dedinaite, A.; Vareikis, A.; Makuska, R.; van der Wal, A.; Furó, I.; Garamus, V. M.; Claesson, P. M., *J. Colloid Interface Sci.* **2007,** *312*, 21.

146. Van de Sande, W.; Persoons, A., *The Journal of Physical Chemistry* **1985,** *89*, 404.

147. Dragan, S.; Cristea, M., *Polymer* **2002,** *43*, 55.

148. Naderi, A.; Claesson, P. M.; Bergström, M.; Dedinaite, A., *Colloids and Surfaces A: Physicochemical and Engineering Aspects* **2005,** *253*, 83.

149. Naderi, A., and Claesson, P.M., *J. Disp. Sci. Techn* **2005,** *26*, 329.

150. Bijelic, G.; Shovsky, A.; Varga, I.; Makuska, R.; Claesson, P. M., *J. Colloid Interface Sci.* **2010,** *348*, 189.

151. Rojas, O. J.; Ernstsson, M.; Neuman, R. D.; Claesson, P. M., *Langmuir* **2002,** *18*, 1604.

152. Shovsky, A.; Bijelic, G.; Varga, I.; Makuska, R.; Claesson, P. M., *Langmuir* **2011,** *27*, 1044.

153. Dijt, J. C.; Cohen Stuart, M. A.; Fleer, G. J., *Macromolecules* **1992,** *25*, 5416.

154. Dijt, J. C.; Cohen Stuart, M. A.; Fleer, G. J., *Macromolecules* **1994,** *27*, 3207.

155. Karim, K.; Taylor, J. D.; Cullen, D. C.; Swann, M. J.; Freeman, N. J., *Anal. Chem.* **2007,** *79*, 3023.

156. Glaser, R. W., *Anal. Biochem.* **1993,** *213*, 152.

157. Plunkett, K. N.; Zhu, X.; Moore, J. S.; Leckband, D. E., *Langmuir* **2006,** *22*, 4259.

158. Filippov, L. K.; Filippova, N. L., *J. Colloid Interface Sci.* **1997,** *189*, 1.

159. Dijt, J. C.; Cohen Stuart, M. A.; Fleer, G. J., *Macromolecules* **1994,** *27*, 3219.

160. Linse, P.; Claesson, P. M., *Macromolecules* **2009,** *42*, 6310.

7. ACKNOWLEDGEMENTS

I am most thankful to my thesis advisor, Prof. Per Claesson, for giving me the opportunity to carry out this work, for his guidance, scientific supervision, patience and encouragement throughout these years. Through your valuable critique and feed back, I have seen myself become more motivated and more self-confident. For all of that I am forever grateful.
Käre Per! Ett stort tack!

I am also deeply grateful to my co-supervisor, Assoc. Prof. Dr. Imre Varga, who provided guidance during my very first year. His positive attitude, resourcefulness, scientific support and enlightening discussions were always a strong source of motivation. I would like to thank Goran Bijelic for his valuable contribution to the research presented in Paper III in this thesis. Dr. Ali Naderi, I appreciate much your constructive comments on my manuscripts, inspiring and fruitful scientific discussions.

Senior scientists, Mark, Andra, Eva and Magnus are acknowledged for interesting graduate courses and for all kind of help.

Special thanks go to my Swedish friend Rasmus, whose encyclopedical knowledge of various subjects e.g. history, geography, politics, geo-politics etc are just amazing. Thank you for Swedish lessons, for indeed pleasant and interesting discussions which were always a great source of emotional recreation, especially after unsuccessful experimental struggling.

Olga is warmly thanked for keeping up a positive emotional atmosphere, for moral and professional support and for sharing the miseries and joys of the lab life! I also thank Yuliya for enjoyable coffee breaks, during the preparation of this thesis.

During these four years I have been lucky to meet a lot of interesting people. Thank you all for a friendly and pleasant working atmosphere, but also for cheerful hangouts and unforgettable moments: VIP customers of ‘Man in the Moon’ Joseph, Niklas, Goran, Ali,

Mohanty, Esben, Maria, Clayton, Hiro, Emily, Olga, and the most nice people Andra, Yulia S, David, Gunnar, Jonathan, Zsombor, Luba, Arindam, Eric, Petru and Geoffrey. All of you have a special place in my memory.

I wish the best of luck to all former and new colleagues in the division.

Last and not the least, I would like to thank my family and my parents for their unwavering supports throughout these years. I thank my dear wife, Galyna, for her love and support, in my good and especially bad times, and for having given me the most precious gift, our son, Ivan.